Critical dynamics of gelation

Kurt Broderix,* Henning Löwe, Peter Müller, and Annette Zippelius
Institut für Theoretische Physik, Georg-August-Universität, D-37073 Göttingen, Germany
(Received 6 July 2000; published 27 December 2000)

Shear relaxation and dynamic density fluctuations are studied within a Rouse model, generalized to include the effects of permanent random crosslinks. We derive an exact correspondence between the static shear viscosity and the resistance of a random resistor network. This relation allows us to compute the static shear viscosity exactly for uncorrelated crosslinks. For more general percolation models, which are amenable to a scaling description, it yields the scaling relation $k=\phi-\beta$ for the critical exponent of the shear viscosity. Here β is the thermal exponent for the gel fraction, and ϕ is the crossover exponent of the resistor network. The results on the shear viscosity are also used in deriving upper and lower bounds on the incoherent scattering function in the long-time limit, thereby corroborating previous results.

DOI: 10.1103/PhysRevE.63.011510 PACS number(s): 61.25.Hq, 64.60.Ht, 61.20.Lc

I. INTRODUCTION

The most prominent critical phenomena at the gelation or vulcanization transition are of dynamic origin; see e.g., Ref. [1] for a recent review. Relaxation times in the sol phase diverge as the gelation transition is approached [2], giving rise to critical behavior of the transport coefficients: The effective diffusion constant goes to zero and the static shear viscosity diverges [3,2], indicating structural arrest of a macroscopic fraction of the monomers; see Fig. 1 below for a graphical illustration of the situation. There are strong precursors of the gelation transition in the fluidlike sol phase: The decay of correlations is not exponential, but follows a Kohlrausch law [2]. This indicates a spectrum of relaxation times extending to arbitrary large values.

All these phenomena are reminiscent of the glass transition, so that the gelation transition can be regarded as a paragon for the latter. However there are important differences which are best explained in the context of vulcanization. In this case the distinction between thermal and quenched degrees of freedom is simple and unambiguous: Chemical crosslinks are quenched, and the monomers equilibrate in a fixed crosslink configuration. In contrast to this scenario, the quench in the structural glass by lowering the temperature does not allow for such a simple classification. Even though it is generally believed that while decreasing the temperature at a finite rate ω some degrees of freedom are quenched, namely, those whose relaxation times τ are larger than the inverse quench rate, $\tau\omega>1$. Nevertheless the identification of these quenched degrees of freedom is neither simple nor unique, and some properties of structural glasses do in fact depend on the rate of quench [4]. The so-called physical gelation seems a better candidate to model glassy behavior. In this case the temperature can be easily adjusted so that the binding energy for two monomers participating in a crosslink is comparable to the thermal energy. Crosslinks form and break up so that both monomer positions and crosslinks equilibrate. By lowering the temperature crosslinks are quenched, and give rise to structural arrest at sufficiently low temperatures.

In this paper we will concentrate on vulcanization and chemical gelation, both of which are commonly interpreted as a percolation transition [5]. The transition from a fluid phase to an amorphous solid phase happens when a macroscopic cluster of crosslinked polymers has been formed. However, percolation theory can only account for the geometric connectivity of the macromolecules, and neither thermal fluctuations nor dynamic phenomena are comprised in the percolation picture. Instead, one should start from a dynamic model, as is done here. The simplest model, Rouse dynamics, ignores all interactions except for those which ensure the connectivity of the clusters. de Gennes [6] was the first to estimate the static shear viscosity near the gelation transition. Relating the viscosity $\eta(n)$ of a cluster of mass n to the longest relaxation time of the cluster, he argued that $\eta(n)\sim R^2$ scales like the squared linear dimension of the cluster. The radius of gyration is determined by the mass of the cluster according to $R\sim n^{1/d_f}$, where $d_f=d-\beta/\nu$ is the

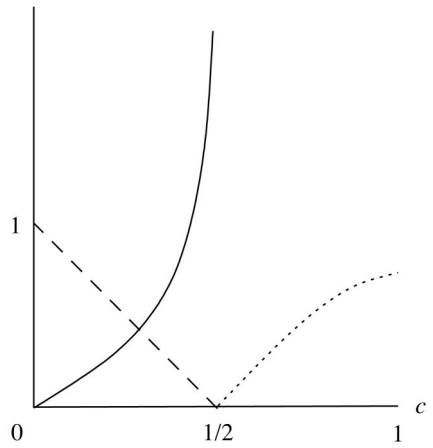

FIG. 1. Sketch of some critical quantities for gelation as a function of the crosslink concentration c for a mean-field distribution of crosslinks. The gelation transition occurs at $c_{\mathrm{crit}}=\frac{1}{2}$. The plot displays the averaged static shear viscosity (solid line) according to Eq. (3.26), the effective diffusion constant (dashed line) according to Eq. (4.17) and the gel fraction (dotted line) according to Ref. [8].

*Deceased (12 May 2000).

Hausdorff-Besicovitch dimension of the fractal, and related to the exponent for the correlation length ν and the gel fraction β. Given a scaling ansatz [7] for the number of n clusters per polymer, $\tau_n \sim n^{-\tau} \exp\{-n/n^*\}$, with $n^* \sim |p-p_c|^{-1/\sigma}$, one can average over all cluster sizes to obtain $\eta = \Sigma_n \eta(n) n \tau_n \sim |p-p_c|^{-k}$, with $k = 2\nu - \beta$. This scaling relation was rederived in many other ways. It is incorrect because it ignores the internal structure of percolation clusters which is not only determined by the exponents β and ν. The latter rule the behavior of clusters on large spatial scales, whereas the intrinsic self-similar connectivity is characterized by the spectral dimension d_s. In contrast to a linear chain with $d_s = 1$, a percolation cluster contains a hierarchy of branches and possibly loops, giving rise to a value of $d_s > 1$. Apparently, Cates [9] was the first to notice that the relaxation spectrum acquires a Lifshits tail which modifies the above estimate for the viscosity $\eta(n)$ of a single percolation cluster.

In a different approach, the viscosity at the sol-gel transition has been related to the conductivity of a random resistor network [10] which is made up of a fraction p of superconducting and a fraction $(1-p)$ of normal conducting bonds. Approaching the percolation transition from below, the conductance $\sigma \sim |p-p_c|^{-s}$ is expected to diverge with an exponent s, which was predicted to be the same as k. Before it was realized that percolation clusters are multifractals, the two scaling arguments were considered to give identical results, namely, $k = s = 2\nu - \beta$. If multifractality is treated properly, the two scaling arguments give different results. This is most easily seen in two dimensions, where duality [11] implies $s = \phi$. Here, ϕ is the so-called crossover exponent, which cannot be expressed through β and ν. It was computed by Harris and Lubensky [12] in the context of random resistor networks, where a fraction $1-p$ of normal conducting bonds was removed. The crossover exponent ϕ characterizes the average resistance $\Omega(r) \sim r^{\phi/\nu}$ between two connected nodes, which are a distance r apart.

In this paper we concentrate on the fluidlike sol phase of a gelling polymer melt. We show that for Rouse dynamics the exponent of the static shear viscosity k is given exactly by

$$k = \phi - \beta \tag{1.1}$$

in disagreement with *both* the above scaling arguments. The derivation of the exponent k requires two steps. First, the viscosity is expressed in terms of the random connectivity matrix, which characterizes the connections in the polymer network. In a second step we prove that bonds between monomers can be identified with electrical resistors, and use results from the theory of random graphs to relate matrix elements of the connectivity matrix to the resistance between two nodes i and j of the corresponding random resistor network. In fact, we consider the derivation of such a correspondence as one of the main results of this paper.

For a mean-field distribution of crosslinks we compute the static shear viscosity exactly and find a logarithmic divergence, in agreement with the general scaling relation (1.1) for mean-field exponents or space dimensionality $d \geqslant 6$. For a crosslink distribution which corresponds to finite-dimensional percolation, we know the ϵ expansion of $k = \epsilon/6 + 11\epsilon^2/1764 + O(\epsilon^3)$, or use high-precision simulations in $d=3$ to obtain $k|_{d=3} \approx 0.71$.

The established correspondence between the random polymer network and the random resistor network also turns out to be useful for a computation of the intermediate incoherent scattering function $S_t(q)$. The long-time asymptotics of $S_t(q)$ was discussed in Ref. [8] for a mean-field distribution of crosslinks. In this paper, we derive upper and lower bounds on $S_t(q)$ which put our previous results on a firmer basis. We furthermore use a scaling analysis to extract the long-time asymptotics of $S_t(q)$ for a crosslink distribution which corresponds to finite-dimensional percolation.

The paper is organized as follows: In Sec. II, we introduce the basic dynamic model of a monodisperse sol of phantom monomer chains, which are permanently crosslinked by Hookean springs chosen at random [13]. We present a formal solution of the dynamic model, and introduce the two observables, which we want to discuss: the stress relaxation function and the incoherent scattering function. In Sec. III, we discuss the static shear viscosity. First, the relation between our dynamic model and random resistor networks is established. Second, we relate the critical exponent of the viscosity to the exponents arising in a scaling description of the crosslink distribution, as exists for finite-dimensional percolation. Third, we show how to compute the static shear viscosity exactly for the case where the crosslinks are distributed according to mean-field percolation. This result is then rederived using replicas in the last subsection of Sec. III. The intermediate incoherent scattering function is discussed in Sec. IV. We first derive exact upper and lower bounds, which are then used to extract the long-time asymptotics for a mean-field distribution of crosslinks and corroborate previous results [8]. Some details of this calculation are delegated to the Appendix. In the last part of Sec. IV we compute critical exponents associated with the long-time asymptotics of the scattering function for a crosslink distribution which admits a scaling description—as is the case for finite-dimensional percolation. We conclude with some remarks and perspectives for future directions in Sec. V. A brief account of our results was given in Ref. [14].

II. DYNAMIC MODEL AND ITS SOLUTION

A. Dynamic model

We consider a system of N identical, monodisperse (macro)molecular units, each consisting of L monomers. These units may be monomers, dimers, linear chains, or arbitrary branched structures, which may also contain loops. In the following these molecular units are called polymers, regardless of their topology or their degree of polymerization L. Monomer s on polymer i is characterized by its time-dependent position vector $\mathbf{R}_t(i,s)$ $(i = 1, \ldots, N$ and $s = 1, \ldots, L)$ in d-dimensional space. We suppose that the polymers are subjected to a space- and time-dependent external velocity field $v_t^{\alpha}(\mathbf{r})$. Here Greek indices indicate Car-

tesian coordinates $\alpha=x,y,z,\ldots$, and we will always consider a flow field in the r^x direction, increasing linearly with r^y, i.e.,

$$v_t^\alpha(\mathbf{r}) := \delta_{\alpha,x}\kappa_t r^y, \tag{2.1}$$

with a time-dependent shear rate κ_t. As usual, $\delta_{\alpha,\beta}$ denotes the Kronecker symbol, i.e., $\delta_{\alpha,\beta}=1$ for $\alpha=\beta$, and is zero otherwise.

We employ the simplest, purely relaxational dynamics (see, e.g. Chap. 4 in Ref. [15] or Chap. 15.1 in Ref. [16])

$$\partial_t R_t^\alpha(i,s) = -\frac{1}{\zeta}\frac{\partial H}{\partial R_t^\alpha(i,s)} + v_t^\alpha[\mathbf{R}_t(i,s)] + \xi_t^\alpha(i,s). \tag{2.2}$$

In the absence of the thermal noise $\boldsymbol{\xi}$, the monomers relax to the state $\partial H/\partial \mathbf{R}=\mathbf{0}$ such that their velocity is equal to the externally imposed velocity field. The noise $\boldsymbol{\xi}$ has zero mean and covariance $\overline{\xi_t^\alpha(i,s)\xi_{t'}^\beta(i',s')} = 2\zeta^{-1}\delta_{\alpha,\beta}\delta_{i,i'}\delta_{s,s'}\delta(t-t')$, where $\delta(t)$ is the Dirac δ function. Here, the overbar indicates the average over the realizations of the Gaussian noise $\boldsymbol{\xi}$. The relaxation constant is denoted by ζ, and we use energy units such that $k_BT=1$. In Eq. (2.2) the Hamiltonian $H := H_W + U$ consists of two terms. The first one guarantees the connectivity of each polymer, whose internal structure is characterized by a connectivity matrix $\Gamma_{\text{poly}}(s;s')$:

$$H_W := \frac{d}{2l^2}\sum_{i=1}^{N}\sum_{s,s'=1}^{L}\Gamma_{\text{poly}}(s;s')\mathbf{R}(i,s)\cdot\mathbf{R}(i,s'). \tag{2.3}$$

We have chosen a harmonic potential to constrain the relative distance between two monomers on the same polymer with the typical distance given by the persistence length $l>0$. As an example for Γ_{poly}, we mention the special case of linear chains. Their connectivity matrix is explicitly given by

$$\Gamma_{\text{poly}}(s;s') = \sum_{r=1}^{L-1}(\delta_{s,r}-\delta_{s,r+1})(\delta_{s',r}-\delta_{s',r+1}). \tag{2.4}$$

The second part of the Hamiltonian models M permanently formed crosslinks between randomly chosen pairs of monomers. The configuration of crosslinks will be denoted by $\mathcal{G}=\{i_e,s_e;i_e',s_e'\}_{e=1}^M$, i.e., the list of the M crosslinked pairs of monomers. The relative distances between any two monomers, participating in a crosslink, are constrained by a harmonic potential

$$U := \frac{d}{2a^2}\sum_{e=1}^{M}[\mathbf{R}(i_e,s_e)-\mathbf{R}(i_e',s_e')]^2, \tag{2.5}$$

whose strength is controlled by the parameter $a>0$. For $a\to 0$ hard crosslinks can be recovered [13]. Since the Hamiltonian is quadratic in the monomer positions, it can be expressed in terms of a $NL\times NL$ connectivity matrix Γ according to

$$H = \frac{d}{2a^2}\sum_{i,i'=1}^{N}\sum_{s,s'=1}^{L}\Gamma(i,s;i',s')\mathbf{R}(i,s)\cdot\mathbf{R}(i',s'). \tag{2.6}$$

The connectivity matrix Γ has a deterministic part Γ_{poly}, which reflects the internal structure of the polymers, and a random part representing the crosslinks

$$\begin{aligned}\Gamma(i,s;i',s') = {}& \frac{a^2}{l^2}\delta_{i,i'}\Gamma_{\text{poly}}(s,s') \\ & + \sum_{e=1}^{M}(\delta_{i,i_e}\delta_{s,s_e}-\delta_{i,i_s'}\delta_{s,s_e'}) \\ & \times(\delta_{i',i_e}\delta_{s',s_e}-\delta_{i',i_e'}\delta_{s',s_e'}).\end{aligned} \tag{2.7}$$

In order to determine the model completely, it only remains to specify the probability distribution of the crosslink configurations. We shall discuss two different types of probability distributions $P(\mathcal{G})$: (i) crosslinks are chosen independently with equal probability for every pair of monomers, corresponding to a mean-field distribution [17,18]; and (ii) a distribution of crosslinks, which generates clusters amenable to the scaling description of finite-dimensional percolation. A precise characterization of these distributions is given below.

B. Observables

We shall focus on two observables. First, we aim at a computation of the intrinsic shear stress $\sigma_t^{\alpha,\beta}$ as a function of the shear rate κ_t. Following Chap. 3 in Ref. [15] or Chap. 16.3 in Ref. [16], we express the shear stress in terms of the force per unit area, exerted by the polymers

$$\sigma_t^{\alpha,\beta} = \lim_{t_0\to-\infty} -\frac{\rho_0}{N}\sum_{i=1}^{N}\sum_{s=1}^{L}\overline{F_t^\alpha(i,s)R_t^\beta(i,s)}. \tag{2.8}$$

Here $\mathbf{R}_t(i,s)$ is the solution of the equation of motion (2.2) with some initial condition $\mathbf{R}_{t_0}(i,s)$ at time t_0 in the distant past. Moreover, ρ_0 stands for the polymer concentration, and $F_t^\alpha(i,s) := -\partial H/\partial R_t^\alpha(i,s)$ is the force acting on monomer (i,s) at time t. For the simple shear flow [Eq. (2.1)], a linear response relation

$$\sigma_t^{x,y} = \int_{-\infty}^{t} d\tau\, G_{t-\tau}\kappa_\tau, \tag{2.9}$$

with response function G_t, will be shown to be valid for arbitrary strengths of the shear rate κ_t. For a time-independent shear rate κ the shear stress is also independent of time, and the intrinsic shear viscosity η is then related to the shear stress via

$$\eta(\mathcal{G}) := \sigma^{x,y}/(\kappa\rho_0) = \rho_0^{-1}\int_0^\infty dt\; G_t. \tag{2.10}$$

Note that we have made the dependence of η on the realization $\mathcal{G}$ of the crosslinks explicit.

Second, in the absence of the shear flow, $\kappa=0$, we compute the intermediate incoherent scattering function

$$S_t(q|\mathcal{G}) := \lim_{t_0\to-\infty} \overline{\frac{1}{NL}\sum_{i=1}^{N}\sum_{s=1}^{L} \exp\{i\mathbf{q}\cdot[\mathbf{R}_t(i,s)-\mathbf{R}_0(i,s)]\}}, \tag{2.11}$$

with special emphasis on its long-time behavior. Due to isotropy the scattering function depends only on the modulus $q:=|\mathbf{q}|$ of the wave vector.

We expect that observables, like the viscosity and the incoherent scattering function, are self averaging in the macroscopic limit, and compute the averages

$$\langle \eta\rangle := \sum_{\mathcal{G}} P(\mathcal{G})\,\eta(\mathcal{G}) \tag{2.12}$$

and, accordingly, $\langle S_t(q)\rangle$ over all crosslink realizations.

C. Formal solution

The equation of motion (2.2) is linear for the spatially homogeneous shear gradient (2.1), and hence can be solved exactly. For notational convenience we introduce NL-dimensional vectors such as $R_t^\alpha := (R_t^\alpha(1,1),\ldots,R_t^\alpha(N,L))$, whose NL components are the respective spatial components of the position vectors $\mathbf{R}_t(i,s)$. The force vectors $F_t^\alpha = -(d/a^2)\Gamma R_t^\alpha$ and the noise vectors ξ_t^α, $\alpha=x,y,z,\ldots$ are defined in an analogous manner. Furthermore we use the abbreviation $K_t^{\alpha,\beta}=\delta_{\alpha,x}\delta_{\beta,y}\kappa_t$ for the spatial components of the velocity gradient tensor, which according to Eq. (2.1), is spatially homogeneous.

Expression (2.8) for the stress tensor can be rewritten as

$$\begin{aligned}\sigma_t^{\alpha,\beta} &= \frac{\rho_0 d}{Na^2}\lim_{t_0\to-\infty}\mathrm{Tr}(\Gamma C_t^{\alpha,\beta})\\ &= \frac{\rho_0 d}{Na^2}\lim_{t_0\to-\infty}\sum_{i=1}^{N}\sum_{s=1}^{L}(\Gamma C_t^{\alpha,\beta})(i,s;i,s),\end{aligned} \tag{2.13}$$

where $C_t^{\alpha,\beta} := \overline{R_t^\alpha (R_t^\beta)^+}$ is the matrix of second moments of $\mathbf{R}_t$ and the superscript $^+$ denotes transposition. The matrix $C_t^{\alpha,\beta}$ may be calculated from the equation of motion (2.2) as follows: Introducing $U_t(i,s;i',s') := \exp\{-dt/(\zeta a^2)\Gamma\}(i,s;i',s')$, it is readily verified that

$$R_t^\alpha = U_{t-t_0}\sum_\beta T_{t,t_0}^{\alpha,\beta}R_{t_0}^\beta + \int_{t_0}^{t} dt'\,U_{t-t'}\sum_\beta T_{t,t'}^{\alpha,\beta}\xi_{t'}^\beta \tag{2.14}$$

is the unique solution of Eq. (2.2), with initial condition $\mathbf{R}_{t_0}$, provided that $T_{t,t'}^{\alpha,\beta}$ is the solution of the differential equation $\partial_t T_{t,t'}^{\alpha,\beta} = \Sigma_\gamma K_t^{\alpha,\gamma}T_{t,t'}^{\gamma,\beta}$ with initial condition $T_{t,t}^{\alpha,\beta}=\delta_{\alpha,\beta}$. Since $\boldsymbol{\xi}_t$ is Gaussian white noise with zero mean, we obtain

$$\begin{aligned}C_t^{\alpha,\beta} &= U_{2(t-t_0)}\sum_{\gamma,\gamma'} T_{t,t_0}^{\alpha,\gamma}C_{t_0}^{\gamma,\gamma'}T_{t,t_0}^{\beta,\gamma'}\\ &\quad + \frac{2}{\zeta}\int_{t_0}^{t} dt'\,U_{2(t-t')}\sum_\gamma T_{t,t'}^{\alpha,\gamma}T_{t,t'}^{\beta,\gamma}.\end{aligned} \tag{2.15}$$

Multiplying Eq. (2.15) by Γ, and fixing the initial condition at time $t_0\to-\infty$, we end up with

$$\lim_{t_0\to-\infty}\Gamma C_t^{\alpha,\beta} = \frac{2}{\zeta}\int_{-\infty}^{t} dt'\,\Gamma U_{2(t-t')}\sum_\gamma T_{t,t'}^{\alpha,\gamma}T_{t,t'}^{\beta,\gamma}. \tag{2.16}$$

In writing down Eq. (2.16) we have taken advantage of the fact that Γ is a positive semidefinite matrix, implying $\lim_{t\to\infty}U_t=E_0$, where E_0 denotes the orthogonal projector onto the null space of Γ. Inserting Eq. (2.16) into Eq. (2.13), we find an expression for the stress tensor

$$\sigma_t^{\alpha,\beta} = \int_{-\infty}^{t} dt'\left(\frac{d}{dt'}G_{t-t'}\right)\sum_\gamma T_{t,t'}^{\alpha,\gamma}T_{t,t'}^{\beta,\gamma} \tag{2.17}$$

in terms of the time-dependent linear response function

$$G_t = \frac{\rho_0}{N}\mathrm{Tr}\left((1-E_0)\exp\left\{-\frac{2dt}{\zeta a^2}\Gamma\right\}\right). \tag{2.18}$$

As a consequence of the simple shear flow (2.1) we have $T_{t,t'}^{\alpha,\beta}=\delta_{\alpha,\beta}+\delta_{\alpha,x}\delta_{\beta,y}\int_{t'}^{t}d\tau\,\kappa(\tau)$. It follows from definition (2.10) that the static shear viscosity

$$\eta(\mathcal{G}) = \frac{1}{\rho_0}\int_0^\infty dt G_t = \frac{\zeta a^2}{2dN}\mathrm{Tr}\left(\frac{1-E_0(\mathcal{G})}{\Gamma(\mathcal{G})}\right) \tag{2.19}$$

is given by the trace of the Moore-Penrose inverse [19] of Γ, i.e., the inverse of Γ restricted to the subspace of nonzero eigenvalues.

Next we turn to a computation of the incoherent scattering function in the absence of the shear flow. In this case we have $\kappa=0$, and hence $T_{t,t'}^{\alpha,\beta}=\delta_{\alpha,\beta}$. Note that $\mathbf{R}_t-\mathbf{R}_0$ is a Gaussian Markov process whose distribution is characterized in the limit $t_0\to-\infty$ by a vanishing mean and the covariance

$$\lim_{t_0\to-\infty}\overline{(R_t^\alpha-R_0^\alpha)(R_t^\beta-R_0^\beta)^+} = \frac{2}{\zeta}\delta_{\alpha,\beta}\int_0^t d\tau\exp\left\{-\frac{d\tau}{\zeta a^2}\Gamma\right\}. \tag{2.20}$$

To derive Eq. (2.20), we have used solution (2.14). Hence the scattering function is expressed in terms of the diagonal matrix elements of the $NL\times NL$ matrix

$$\begin{aligned}g_t &:= \frac{1}{\zeta}\int_0^t d\tau\exp\left\{-\frac{d\tau}{\zeta a^2}\Gamma\right\}\\ &= \frac{t}{\zeta}E_0 + \frac{a^2}{d}\frac{1-E_0}{\Gamma}\left(1-\exp\left\{-\frac{dt}{\zeta a^2}\Gamma\right\}\right)\end{aligned} \tag{2.21}$$

via

$$S_t(q|\mathcal{G}) = \frac{1}{NL}\sum_{i=1}^{N}\sum_{s=1}^{L}\exp\{-q^2 g_t(\mathcal{G}|i,s;i,s)\}, \tag{2.22}$$

where, again, the dependence on the realization $\mathcal{G}$ has been made explicit.

D. Cluster decomposition

Each crosslink realization $\mathcal{G}$ defines a random labeled graph, which can be decomposed into its maximal pathwise connected components or clusters

$$\mathcal{G}=\bigcup_{k=1}^{K}\mathcal{N}_k. \tag{2.23}$$

Here $\mathcal{N}_k$ denotes the kth cluster with N_k polymers out of a total of K clusters. The associated connectivity matrix, also called the Kirchhoff matrix or admittance matrix in graph theory (see, e.g., p. 54 in Ref. [20]), is of block-diagonal form:

$$\Gamma(\mathcal{G})=\bigoplus_{k=1}^{K}\Gamma(\mathcal{N}_k). \tag{2.24}$$

Therefore the viscosity (2.19) is decomposed into contributions from different clusters according to

$$\eta(\mathcal{G})=\sum_{k=1}^{K}\frac{N_k}{N}\,\eta(\mathcal{N}_k), \tag{2.25}$$

where the individual contribution from cluster $\mathcal{N}_k$ is defined by

$$\eta(\mathcal{N}_k):=\frac{\zeta a^2}{2dN_k}\mathrm{Tr}\left(\frac{1-E_0(\mathcal{N}_k)}{\Gamma(\mathcal{N}_k)}\right). \tag{2.26}$$

In the same way the incoherent scattering function may be decomposed into contributions from different clusters

$$S_t(q|\mathcal{G})=\sum_{k=1}^{K}\frac{N_k}{N}S_t(q|\mathcal{N}_k), \tag{2.27}$$

where the individual contribution from cluster $\mathcal{N}_k$ is defined by

$$S_t(q|\mathcal{N}_k):=\frac{1}{N_kL}\sum_{i\in\mathcal{N}_k}\sum_{s=1}^{L}\exp\{-q^2g_t(\mathcal{N}_k|i,s;i,s)\}. \tag{2.28}$$

Combining Eqs. (2.27), (2.28), and (2.21), we express the scattering function as

$$\begin{aligned}S_t(q|\mathcal{G})=\sum_{k=1}^{K}\frac{N_k}{N}&\exp\left\{-\frac{q^2t}{\zeta N_kL}\right\}\sum_{i\in\mathcal{N}_k}\sum_{s=1}^{L}\frac{1}{N_kL}\\&\times\exp\left\{-\frac{q^2a^2}{d}\left[\frac{1-E_0(\mathcal{N}_k)}{\Gamma(\mathcal{N}_k)}\right.\right.\\&\left.\left.\times\left(1-\exp\left\{-\frac{dt}{\zeta a^2}\Gamma(\mathcal{N}_k)\right\}\right)\right](i,s;i,s)\right\},\end{aligned} \tag{2.29}$$

where we have used the representation

$$E_0(\mathcal{G}|i,s;i',s')=\sum_{k=1}^{K}\frac{1}{N_kL}\,\delta_{\mathcal{N}(i),\mathcal{N}_k}\delta_{\mathcal{N}_k,\mathcal{N}(i')} \tag{2.30}$$

of the orthogonal projector E_0 onto the null space of Γ. Here $\mathcal{N}(i)$ denotes the cluster containing polymer i. Equation (2.30) follows from the fact that the null space of Γ is spanned by vectors which are constant when restricted to any one cluster. Physically this reflects that there is no force acting on the center of mass of any one cluster. Hence the number of zero modes of Γ is equal to the total number K of clusters.

For calculating disorder averages it will be advantageous to reorder the sums in Eqs. (2.25) and (2.29) by first summing over all clusters consisting of a given number n of polymers, and subsequently summing over all ''sizes'' n. Thus we obtain a decomposition of the average

$$\left\langle\sum_{k=1}^{K}\frac{N_k}{N}f(\mathcal{N}_k)\right\rangle=\sum_{n=1}^{\infty}n\,\tau_n\langle f\rangle_n \tag{2.31}$$

for an arbitrary real-valued function f. In Eq. (2.31), we introduce the average

$$\langle f\rangle_n:=\frac{1}{\tau_n}\left\langle\frac{1}{N}\sum_{k=1}^{K}\delta_{N_k,n}\,f(\mathcal{N}_k)\right\rangle \tag{2.32}$$

over all clusters of n polymers, each consisting of L monomers. Furthermore,

$$\tau_n:=\left\langle\frac{1}{N}\sum_{k=1}^{K}\delta_{N_k,n}\right\rangle \tag{2.33}$$

represents the average number of clusters of size n per polymer. Note that up to now no particular crosslink distribution has been specified.

III. SHEAR VISCOSITY

A. Relation to networks of random resistors

The viscosity (2.19) of randomly crosslinked polymers can be quite generally related to the resistance of a random electrical network. Thanks to the cluster decomposition (2.25), it suffices to consider an arbitrary connected cluster $\mathcal{N}_k$. To establish this connection we identify a bond between two neighboring monomers on the same polymer as a resistor of magnitude l^2/a^2, and a crosslink between polymers as a resistor of magnitude 1. The resistance measured between any connected pair of vertices (i,s) and (i',s') will be denoted by $\mathcal{R}(i,s;i',s')$. For an arbitrary connected resistor network $\mathcal{N}_k$ the laws of Ohm and Kirchhoff lead [21] to a relation between $\mathcal{R}$ and the Moore-Penrose inverse of the connectivity matrix:

$$\mathcal{R}(\mathcal{N}_k|i,s;i',s') = \frac{1-E_0(\mathcal{N}_k)}{\Gamma(\mathcal{N}_k)}(i,s;i,s) + \frac{1-E_0(\mathcal{N}_k)}{\Gamma(\mathcal{N}_k)}(i',s';i',s') - 2\frac{1-E_0(\mathcal{N}_k)}{\Gamma(\mathcal{N}_k)}(i,s;i',s'). \quad (3.1)$$

The matrix elements of the projector $E_0(\mathcal{N}_k)$ are all equal to $(N_k L)^{-1}$ according to Eq. (2.30). Hence, when summing Eq. (3.1) over all $(i,s),(i',s') \in \mathcal{N}_k$, the last term on the right-hand side is equal to $-2N_k L\ \mathrm{Tr}[E_0(\mathcal{N}_k)(1-E_0(\mathcal{N}_k))/\Gamma(\mathcal{N}_k)]$, and thus vanishes. Using this fact and definition (2.26) of $\eta(\mathcal{N}_k)$, the viscosity of a cluster $\mathcal{N}_k$ is seen to be given by a sum over resistances

$$\eta(\mathcal{N}_k) = \frac{\zeta a^2}{4dLN_k^2} \sum_{(i,s),(i',s') \in \mathcal{N}_k} \mathcal{R}(\mathcal{N}_k|i,s;i',s'). \quad (3.2)$$

Together with Eq. (2.25), this constitutes the announced connection between the viscosity of a randomly crosslinked polymer melt and a random resistor network. We would like to emphasize that this connection relies on the special form (2.19) of the viscosity in the Rouse model.

B. Finite-dimensional percolation: scaling description

The gelation and the vulcanization transition were interpreted as a percolation transition already by Flory and Stockmayer [22–24]. Even though the classical theories had to be replaced by modern approaches [6,25] built on the analogy to critical phenomena, the percolation picture survived. It is generally believed that the ensemble of macromolecular clusters which are built in the process of gelation has the same statistical connectivity as an ensemble of clusters which are constructed in a *d*-dimensional bond percolation process. This identification is supported by experiment, e.g., the measured cluster-size distribution of macromolecules is well described by the critical exponents predicted for bond percolation [5,7].

The most intuitive picture of gelation and vulcanization is related to continuum percolation, which is expected to be in the same universality class as random bond percolation [5]. In continuum percolation a set of points is randomly distributed in *d*-dimensional space. The points are assumed to be the centers of spheres with randomly distributed radii. Two points are said to be connected if their spheres overlap. Correspondingly, if a crosslinking agent is added to a dense polymer solution or melt, then we expect that pairs of monomers which are close to each other will be crosslinked with high probability, provided the reaction is sufficiently fast as compared to the diffusion time of the polymers.

The well-known characteristics of percolation clusters will allow us to determine the critical behavior of the shear viscosity as given by Eqs. (2.25) and (2.31). For this purpose we first recall some quantities which are important in the scaling theory of percolation; see, e.g., Refs. [7,5]. For definiteness we consider bond percolation on the *d*-dimensional cubic lattice $\mathbb{Z}^d$. Nearest-neighbor bonds are present with probability $p := c/(2d)$, and absent with probability $1-p$. The bonds are interpreted as crosslinks, while the lattice points are identified with monomers. Here the probability p is defined such that the average number of crosslinks is given by $M = cN$. A percolating cluster first appears at a critical crosslink concentration c_{crit}. The fraction Q of lattice points belonging to the infinite network serves as an order parameter, and vanishes continuously as the percolation transition is approached: $Q \overset{c \downarrow c_{\mathrm{crit}}}{\sim} (c-c_{\mathrm{crit}})^{\beta}$. The correlation function $\mathcal{P}(r)$ is proportional to the probability that two vertices which belong to the same cluster are a distance r apart. As the transition is approached, correlations become increasingly long ranged, as is indicated by a divergence of the correlation length ξ:

$$\xi^2 := \sum_{r \in \mathbb{Z}^d} r^2 \mathcal{P}(r) \overset{c \uparrow c_{\mathrm{crit}}}{\sim} (c_{\mathrm{crit}}-c)^{-2\nu}. \quad (3.3)$$

At the critical point the correlation function shows an algebraic decay

$$\mathcal{P}(r)\big|_{c=c_{\mathrm{crit}}} \overset{r \to \infty}{\sim} r^{-(d-2+\eta)}. \quad (3.4)$$

As far as geometric properties of percolation are concerned, the critical behavior is determined by two independent exponents. Here we choose the exponent ν of the correlation length and the anomalous dimension η. The other exponents may be expressed in terms of those via various scaling relations, such as

$$\beta = \frac{\nu}{2}(d-2+\eta). \quad (3.5)$$

It is a well-established fact of the scaling description of percolation that the average number of clusters of size n obeys a scaling law

$$\tau_n = n^{-\tau} f[(c_{\mathrm{crit}}-c)n^{\sigma}], \quad (3.6)$$

with the scaling function f decaying faster than any polynomial for large arguments and approaching a nonzero constant for small arguments. The exponents σ and τ are related to η and ν by

$$\tau = 1 + \frac{2d}{d+2-\eta}, \quad \sigma = \frac{2}{\nu(d+2-\eta)}. \quad (3.7)$$

After these preliminaries we turn to the calculation of the averaged viscosity. For the sake of simplicity we consider polymers with $L=1$, that is, a network of Brownian particles. This is relevant for random networks of macromolecules which are generated by polycondensation, starting from small units without internal structure. Relation (3.2) between the viscosity of a cluster and the corresponding resistance then simplifies to

$$\eta(\mathcal{N}_k)=\frac{\zeta a^2}{4dN_k^2}\sum_{i,i'\in\mathcal{N}_k}\mathcal{R}(\mathcal{N}_k|i;i'). \tag{3.8}$$

We remark that the average $\langle\eta\rangle_n$, which was defined in Eq. (2.32), is an expectation value over all lattice animals of size n, and $N\tau_n$ refers to the average number of percolation clusters of size n.

We make the basic assumption that $\langle\eta\rangle_n$ which, according to Eq. (2.32), only tests clusters of a given finite size n, does not acquire any irregularity as the critical point is approached and that $\langle\eta\rangle_n|_{c=c_{\rm crit}}\sim n^b$ with some yet unknown exponent b. We will see below in Eq. (3.22) that this holds true with $b=1/2$ in the special case where the crosslinks are distributed according to mean-field percolation. Furthermore, we remark that this assumption may be circumvented in a more sophisticated approach, as will be explained below.

Using the properties of the scaling function f and Eq. (3.7), Eqs. (2.25) and (2.31) yield for the asymptotic behavior of the viscosity

$$\langle\eta\rangle \overset{c\uparrow c_{\rm crit}}{\sim}\sum_{n=1}^{\infty}n\tau_n\langle\eta\rangle_n|_{c=c_{\rm crit}}\sim\sum_{n=1}^{\infty}n\tau_n n^b \overset{c\uparrow c_{\rm crit}}{\sim}(c_{\rm crit}-c)^{-A(b)}, \tag{3.9}$$

with a critical exponent $A(b):=\frac{1}{2}b\nu(d+2-\eta)-\frac{1}{2}\nu(d-2+\eta)$. Thus the remaining task is the derivation of the exponent b.

Since the critical behavior of the viscosity is believed not to be determined solely by large-scale geometrical properties, i.e., by the exponents η and ν, the appearance of a new exponent is expected. From Eqs. (3.8) and (2.32) the average over clusters of size n is written in the form

$$\langle\eta\rangle_n=\frac{\zeta a^2}{4dn^2\tau_n}\left\langle\frac{1}{N}\sum_{k=1}^{K}\delta_{N_k,n}\sum_{i,i'=1}^{N}\times\delta_{\mathcal{N}(i),\mathcal{N}_k}\delta_{\mathcal{N}_k,\mathcal{N}(i')}\mathcal{R}(i;i')\right\rangle, \tag{3.10}$$

which yields

$$\frac{4d}{\zeta a^2}\sum_{n=2}^{\infty}n^2\tau_n\langle\eta\rangle_n=\left\langle\frac{1}{N}\sum_{i,i'=1}^{N}\delta_{\mathcal{N}(i),\mathcal{N}(i')}\mathcal{R}(i;i')\right\rangle=\left\langle\sum_{i'\in\mathcal{N}(i)}\mathcal{R}(i;i')\right\rangle \overset{c\uparrow c_{\rm crit}}{\sim}(c_{\rm crit}-c)^{-(2-\eta)\nu-\phi}. \tag{3.11}$$

To obtain the second equality in Eq. (3.11), we used the enumeration invariance of the system, and the asymptotic behavior for $c\uparrow c_{\rm crit}$ is obtained from Eq. (2.45) in Ref. [12]. The exponent ϕ, which was first introduced in the context of random resistor networks, governs [26,12,27] the growth of the resistance $\mathcal{R}(r)$ between two points on the incipient spanning cluster, which are a large spatial distance r apart: $\mathcal{R}(r)\sim r^{\phi/\nu}$. Referred to as the crossover resistance exponent [12,27], ϕ is related [7] to the spectral dimension, according to $\phi=\nu d_f[(2/d_s)-1]$, where $d_f=d-\beta/\nu$ is the Hausdorff-Besicovitch dimension of the incipient spanning cluster. Again using the scaling assumptions (3.6) and $\langle\eta\rangle_n|_{c=c_{\rm crit}}\sim n^b$, Eq. (3.11) amounts to

$$\sum_{n=1}^{\infty}n\tau_n n^{b+1}\overset{c\uparrow c_{\rm crit}}{\sim}(c_{\rm crit}-c)^{-(2-\eta)\nu-\phi}, \tag{3.12}$$

which, upon comparison with Eq. (3.9), gives $A(b+1)=(2-\eta)\nu+\phi$ and, after a little algebra, the relation

$$b=\sigma\phi=(2/d_s)-1. \tag{3.13}$$

Thus we have derived the scaling relation

$$k=\phi-\beta \tag{3.14}$$

for the viscosity exponent k.

As already mentioned, the above scaling assumption is encoded in a more general scaling relation. In Refs. [12] and [27] the authors discussed the generating function

$$Z(\lambda,\omega):=\left\langle\exp\left\{-\frac{\lambda^2}{2}\left(\frac{1}{\Gamma+i\omega}\right)_{j,j}\right\}\right\rangle \tag{3.15}$$

of the distribution of the resolvent of Γ. Among other things, they showed by means of a renormalization-group analysis up to second order in $\varepsilon=6-d$ the validity of the scaling relation

$$Z(\lambda,\omega)\overset{c\uparrow c_{\rm crit}}{\sim}(c_{\rm crit}-c)^{\beta}z[(c_{\rm crit}-c)^{-\phi}\lambda^2,(c_{\rm crit}-c)^{1/\sigma}\omega], \tag{3.16}$$

with an appropriate scaling function z. We use the fact that the system is translationally invariant and relate the viscosity to Z via

$$\langle\eta\rangle=\frac{\zeta a^2}{2d}\left\langle\left(\frac{1-E_0}{\Gamma}\right)_{j,j}\right\rangle=-\frac{\zeta a^2}{d}\lim_{\omega\to0}\frac{\partial}{\partial\lambda^2}\bigg|_{\lambda=0}Z(\lambda,\omega). \tag{3.17}$$

To derive the second equality, we have employed the expansion

$$\frac{1}{\Gamma+i\omega}=-\frac{i}{\omega}E_0+\frac{1-E_0}{\Gamma}+\mathcal{O}(\omega),\quad \omega\to0 \tag{3.18}$$

in Eq. (3.15). From Eq. (3.17), the result (3.14) is readily rederived.

C. Mean-field percolation: exact results

To go beyond scaling arguments and to compute the viscosity for all crosslink concentrations, we have to resort to simpler cluster distributions than the one given by bond percolation in finite-dimensional space. We only consider the simplest distribution which is equivalent to mean-field percolation, as far as static quantities are concerned. All pairs of monomers are equally likely to be crosslinked, and no correlations between crosslinks are taken into account. More precisely, for a function f depending on the realization $\mathcal{G}=\{i_e,s_e;i'_e,s'_e\}_{e=1}^{M}$ of the network we define the average by

$$\langle f\rangle := \lim_{\substack{N,M\to\infty \\ M/N=c}} \left(\prod_{e=1}^{M} \frac{1}{(NL)^2} \sum_{i_e,i'_e=1}^{N} \sum_{s_e,s'_e=1}^{L} \right) \times f(\{i_e,s_e;i'_e,s'_e\}). \tag{3.19}$$

The static shear viscosity can be computed exactly for this simple distribution, making use of results in the mathematical literature on random graphs. The calculations are easiest for a network of Brownian particles, that is, polymers consisting of just one monomer each ($L=1$). The generalization to more complex molecular units with arbitrary L—not necessarily linear—will be shown to be straightforward. It will not change the critical behavior as compared to the case $L=1$.

1. Brownian particles: L=1

The statistical properties of clusters generated according to the above distribution, have been studied extensively in the theory of random graphs, as developed in Ref. [17]. Strictly speaking, the ensemble of random graphs considered in Ref. [17] comprises random labeled graphs consisting of N vertices and $M=cN$ edges, and each of the $\binom{N}{2}_M$ possible graphs is equally likely to occur, i.e., double edges or self-loops are suppressed. Obviously this ensemble differs from the one considered in Eq. (3.19), but one expects both to have the same properties in the macroscopic limit. This may be understood by comparing the number $O(N)$ of possibilities to realize a self-loop or double edge in $\mathcal{G}$ with the number $O(N^2)$ of possibilities to choose a different monomer.

In the macroscopic limit there are no clusters of macroscopic size for $c<c_{\mathrm{crit}}:=\frac{1}{2}$, and all monomers belong to tree clusters without loops, see Theorems (5d) and (5e) in Ref. [17]. Moreover, according to Eq. (2.18) in Ref. [17] one has

$$\tau_n=\frac{n^{n-2}}{2cn!}(2ce^{-2c})^n \tag{3.20}$$

for the average number of trees of size n per polymer. Since each cluster $\mathcal{N}_k$ of size $n=N_k$ is expected to be realized as exactly one of the n^{n-2} labeled trees $\mathcal{T}_n$ of size n, one has $\Sigma_{\mathcal{T}_n}\delta_{\mathcal{N}_k,\mathcal{T}_n}=\delta_{N_k,n}$, and the expectation (2.32) over clusters of size n is expressed as an expectation over trees:

$$\langle f\rangle_n=\sum_{\mathcal{T}_n} f(\mathcal{T}_n)\frac{1}{\tau_n}\left\langle \frac{1}{N}\sum_{k=1}^{K}\delta_{\mathcal{N}_k,\mathcal{T}_n}\right\rangle = \frac{1}{n^{n-2}}\sum_{\mathcal{T}_n} f(\mathcal{T}_n). \tag{3.21}$$

The last step is understood as follows: The assumption that $\mathcal{N}_k$ is a tree of size n fixes the number of vertices and edges in $\mathcal{N}_k$. Hence, due to the independence of the crosslinks in Eq. (3.19), the number of graphs, which may be realized within this assumption, depends only on the size n, and all trees $\mathcal{T}_n$ can be proven to occur equally likely as a realization of $\mathcal{N}_k$. Accordingly, the probability $\tau_n^{-1}\langle N^{-1}\Sigma_{k=1}^{K}\delta_{\mathcal{N}_k,\mathcal{T}_n}\rangle$ for a cluster $\mathcal{N}_k$ of size n to be realized as the tree $\mathcal{T}_n$ is equal to n^{2-n}.

Note further that the resistance between two vertices i and i' in a tree simplifies considerably, because there is a unique path connecting i and i', implying that all resistors are in series. Therefore the resistance $\mathcal{R}(i;i')$ is equal to the number of crosslinks connecting i and i'. Hence we refer to Theorems (1) and (2) in Ref. [28] for computing

$$\langle \mathcal{R}(i;i')\rangle_n=(n-2)!\sum_{\nu=2}^{n}\frac{n^{1-\nu}\nu(\nu-1)}{(n-\nu)!}\overset{n\to\infty}{\sim}\sqrt{n\pi/2},\quad i\neq i'. \tag{3.22}$$

Obviously, one has $\langle \mathcal{R}(i,i)\rangle_n=0$. Now Eqs. (3.2) and (3.22) imply

$$\langle \eta\rangle_n=\frac{\zeta a^2}{4d}(n-1)!\sum_{\nu=2}^{n}\frac{n^{-\nu}\nu(\nu-1)}{(n-\nu)!}. \tag{3.23}$$

Combining Eqs. (2.25), (2.31) and (3.23), and expanding the exponential in Eq. (3.20), one obtains

$$\begin{aligned}\langle \eta\rangle &= \frac{\zeta a^2}{8dc}\sum_{n=2}^{\infty}\sum_{l=0}^{\infty}\sum_{\nu=2}^{n}(-1)^l\frac{(2c)^{n+l}n^{n+l-\nu-2}\nu(\nu-1)}{l!(n-\nu)!}\\ &= \frac{\zeta a^2}{8dc}\sum_{j=2}^{\infty}(2c)^j\sum_{l=0}^{j-2}\sum_{\nu=2}^{j-l}(-1)^l\frac{(j-l)^{j-\nu-2}\nu(\nu-1)}{l!(j-l-\nu)!}\\ &= \frac{\zeta a^2}{8dc}\sum_{j=2}^{\infty}(2c)^j\sum_{\nu=2}^{j}\frac{\nu(\nu-1)}{(j-\nu)!}\\ &\quad\times\sum_{l=0}^{j-\nu}(-1)^l(j-l)^{j-\nu-2}\binom{j-\nu}{l}.\end{aligned} \tag{3.24}$$

To sum up this expression in closed form, we note that

$$\begin{aligned}\sum_{l=0}^{m}(-1)^l(\alpha+m-l)^{m-2}\binom{m}{l}&\\ =\begin{cases}\alpha^{-2}, & \text{for } m=0\\ -(\alpha(\alpha+1))^{-1}, & \text{for } m=1\\ 0, & \text{otherwise}\end{cases}&\end{aligned} \tag{3.25}$$

For $m=0$ and 1, this is verified by inspection, and for $m\geqslant 2$ it is verified by differentiating formula 0.154.5 in Ref.

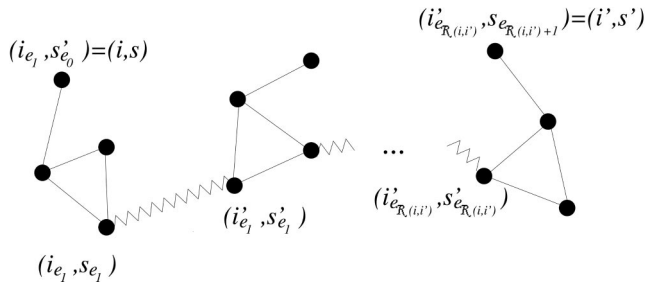

FIG. 2. Contributions to the total resistance in Eq. (3.28). Crosslinks are depicted as zigzag lines, and intrapolymer bonds as straight lines.

[29] twice with respect to α. Hence the result of the ν and l sums in Eq. (3.24) is equal to $1/j$, and we obtain

$$\langle \eta \rangle = \frac{\zeta a^2}{8dc}\left[\ln\left(\frac{1}{1-2c}\right) - 2c\right], \quad \text{for } L=1 \tag{3.26}$$

for the averaged viscosity for all $0<c<\frac{1}{2}$. The viscosity exhibits a logarithmic divergence at the critical concentration $c_{\text{crit}}=\frac{1}{2}$, corresponding to the critical exponent $k=0$. This is in accordance with the more general result (3.14) because for $d \geqslant 6$ one has $\beta=1=\phi$ [7]. The behavior (3.26) of the averaged viscosity is displayed in Fig. 1.

2. Network of polymers: General L

The result (3.26) is readily generalized to networks of crosslinked polymers, all having the same number $L \geqslant 1$ of monomers and the same geometric structure. The only difference is that now there are two different kinds of resistors with magnitudes l^2/a^2 and 1, corresponding to intrapolymer bonds and crosslinks, respectively. Due to the fact that the monomer labels s are distributed independently from the chain labels i in the expectation (3.19), it follows by the same arguments as above that in the macroscopic limit all polymers are connected within tree clusters $\{i_e, i'_e\}$. Thus the average (3.21) over all possible configurations of clusters consisting of n polymers generalizes to

$$\langle f \rangle_n = \left(\prod_{e=1}^{n-1} \frac{1}{L^2} \sum_{s_e, s'_e=1}^{L} \right) \frac{1}{n^{n-2}} \sum_{\mathcal{T}_n} f(\{i_e, s_e; i'_e, s'_e\}). \tag{3.27}$$

In Eq. (3.27) the average is taken over equally probable trees $\mathcal{T}_n = \{i_e, i'_e\}_{e=1}^n$ and over independently chosen, equally probable, monomer labels. Given $i, i' \in \mathcal{T}_n$, the resistance $\mathcal{R}(i,s;i',s')$ splits up into two additive contributions; see also Fig. 2. The first is the crosslink part $\mathcal{R}(i;i')$, which is equal to the number of interpolymer crosslinks, that is resistors of magnitude one, on the unique path on the tree $\mathcal{T}_n$ from i to i'. Let us denote these crosslinks by $\{i_{e_k}, s_{e_k}; i'_{e_k}, s'_{e_k}\}_{k=1}^{\mathcal{R}(i,i')}$. The second stems from intrapolymer resistors of magnitude l^2/a^2. Thus we write

$$\mathcal{R}(i,s;i',s') = \mathcal{R}(i,i') + \frac{l^2}{a^2} \sum_{k=0}^{\mathcal{R}(i,i')} \mathcal{Q}(s'_{e_k}, s_{e_{k+1}}), \tag{3.28}$$

where $s'_{e_0} := s$, $s_{e_{\mathcal{R}(i,i')+1}} := s'$ and $(l^2/a^2)\mathcal{Q}(\sigma,\sigma')$ is the resistance measured between monomer σ and monomer σ' on the same polymer. It follows that

$$\frac{1}{L^2} \sum_{s,s'=1}^{L} \left\langle \sum_{k=0}^{\mathcal{R}(i,i')} \mathcal{Q}(s'_{e_k}, s_{e_{k+1}}) \right\rangle_n = (1 + \langle \mathcal{R}(i,i') \rangle_n) \mathcal{Q}_L. \tag{3.29}$$

The latter holds due to the fact that monomer and polymer labels are distributed independently in the average (3.27), and we have introduced the averaged single-polymer resistance

$$\mathcal{Q}_L := \frac{1}{L^2} \sum_{\sigma,\sigma'=1}^{L} \mathcal{Q}(\sigma,\sigma'). \tag{3.30}$$

Upon inserting Eq. (3.28) into Eq. (3.2), these two relations lead to

$$\langle \eta \rangle_n = L\left(1 + \frac{l^2}{a^2}\mathcal{Q}_L\right) \langle \eta \rangle_n|_{L=1} + \frac{\zeta l^2}{4d} L \mathcal{Q}_L. \tag{3.31}$$

Thus the averaged viscosity for general $L \geqslant 1$ follows from Eqs. (2.31) and (3.31), the averaged viscosity (3.26) of the corresponding Brownian-particle case, and the relation $\Sigma_{n=1}^{\infty} n \tau_n = 1$, which is valid for all $0<c<\frac{1}{2}$. This gives rise to the exact result

$$\langle \eta \rangle = \frac{\zeta a^2}{8cd} L\left(1 + \frac{l^2}{a^2}\mathcal{Q}_L\right)\left[\ln\left(\frac{1}{1-2c}\right) - 2c\right] + \frac{\zeta l^2}{4d} L \mathcal{Q}_L \tag{3.32}$$

for the averaged viscosity of a crosslinked polymer melt on the sol side. As in the Brownian-particle case, it exhibits a logarithmic divergence at the critical crosslink concentration $c_{\text{crit}}=\frac{1}{2}$. The result (3.32) is universal in the sense that the details of the model only affect the prefactor of the critical divergence. The prefactor depends on the persistence length l and the ''extension'' of the crosslinks a, as well as on the number L of monomers of a polymer and on the geometric structure of a polymer through the averaged single-polymer resistance $\mathcal{Q}_L$. Let us mention three concrete examples for the latter. First, in the special case where the polymers are chain molecules, the averaged single-polymer resistance is given by $\mathcal{Q}_L = L^{-2}\Sigma_{\sigma,\sigma'=1}^{L}|\sigma-\sigma'| = (L^2-1)/(3L)$. Accordingly, for long chains, the viscosity is proportional to L^2, as it should be within a Rouse-type model [15]. Second, for ring polymers, $\mathcal{Q}_L = (L^2-1)/(6L)$ is half as large as for linear chains. Third, for star polymers, one obtains $\mathcal{Q}_L = 2(L-1)^2/L^2$, which implies a linear growth of $\langle \eta \rangle$ in L for large L. In all three cases the scaling of the prefactor with L in (3.32) is not altered when passing to the limit $a \downarrow 0$ of hard crosslinks.

D. Alternative derivation with replicas

In this section we rederive the result (3.26) for the disorder average of the viscosity of a network of Brownian particles by means of the replica trick. We consider the mean-field distribution of crosslinks, where each crosslink (i,i'), $1 \leqslant i < i' \leqslant N$, occurs independently with probability $2c/N$. In many respects this ensemble is equivalent in the macroscopic limit to the one with a fixed number of crosslinks, which underlies (3.26), and was defined by the expectation (3.19) for $L=1$. In particular, $c_{\rm crit}=\frac{1}{2}$ and the expression (3.20) for the average number τ_n of trees of size n per polymer remain valid, as can be inferred from Theorems V.7 and V.5 in Ref. [30]. Additionally, Eq. (3.21) continues to hold, because the crosslinks are distributed independently and with equal probabilities. Therefore, the averaged viscosity is given by Eq. (3.26) for both ensembles.

In this subsection we focus again on the non-percolating regime $c<c_{\rm crit}=\frac{1}{2}$. To leading order in $N \gg 1$ the ensemble, where the crosslinks are distributed with probability $2c/N$, is characterized by the characteristic function

$$\langle e^{\mathrm{Tr}(\Gamma A)} \rangle = \exp\left\{ \frac{c}{N} \sum_{i,i'=1}^{N} e^{A_{i,i}+A_{i',i'}-A_{i,i'}-A_{i',i}} - cN \right\} \tag{3.33}$$

of the connectivity matrix Γ. Here A denotes an arbitrary $N \times N$ matrix. Note that, contrary to our previous conventions, in this subsection we do not include the limit $N \to \infty$ in the average $\langle \bullet \rangle$. The ensemble (3.33) of random matrices is closely related to that in Ref. [31], where the density of states of Γ was investigated with the replica trick; see also Refs. [32] and [33] for recent works devoted to this issue.

The following computation of $\langle \eta \rangle$ with replicas has a lot in common with that of the density of states in Ref. [31]. Therefore we have chosen a less detailed exposition in this subsection and only concentrate on the main steps. Compared to Ref. [31] there is one large difference, however. For the purpose of $\langle \eta \rangle$ one can solve the resulting saddle-point equation exactly by analytic means.

The basic quantity in the replica calculation is the averaged resolvent or Green function

$$\begin{aligned} G(\Omega) &:= \lim_{N\to\infty} \frac{1}{2N} \left\langle \mathrm{Tr}\left(\frac{1}{\Gamma+\Omega} \right) \right\rangle \\ &= \lim_{N\to\infty} \frac{1}{2N} \left(\left\langle \mathrm{Tr}\left(\frac{1-E_0}{\Gamma+\Omega} \right) \right\rangle + \frac{1}{\Omega} \langle \mathrm{Tr}(E_0) \rangle \right) \end{aligned} \tag{3.34}$$

of Γ, in terms of which the viscosity (2.19) is written as

$$\begin{aligned} \lim_{N\to\infty} \langle \eta \rangle &= \frac{\zeta a^2}{d} \lim_{\Omega\to 0} \left(G(\Omega) - \lim_{N\to\infty} \frac{\langle \mathrm{Tr}(E_0) \rangle}{2N\Omega} \right) \\ &= \frac{\zeta a^2}{d} \lim_{\Omega\to 0} \left(G(\Omega) - \frac{1-c}{2\Omega} \right). \end{aligned} \tag{3.35}$$

To obtain the second equality in Eq. (3.35), we use the fact that the dimensionality of the null space of Γ is equal to the total number of clusters, and refer to Theorems V.7(ii) and V.12 in Ref. [30]. In the following we compute $G(\Omega)$ with replicas, and show that it has a singular contribution for $\Omega \to 0$ which cancels the second term in Eq. (3.35). The regular part of $G(\Omega)$ determines the viscosity.

Introducing the generating function

$$\begin{aligned} Z_N(\Omega) &:= \int_{\mathbb{R}^N} \left(\prod_{i=1}^{N} \frac{dx_i}{\sqrt{2\pi}} \right) \\ &\quad \times \exp\left(-\frac{1}{2} \sum_{i,i'=1}^{N} x_i x_{i'} (\Gamma_{i,i'} + \Omega \delta_{i,i'}) \right), \end{aligned} \tag{3.36}$$

the resolvent (3.34) is expressed as

$$G(\Omega) = -\lim_{N\to\infty} \frac{1}{N} \left\langle \frac{\partial \ln Z_N(\Omega)}{\partial \Omega} \right\rangle. \tag{3.37}$$

Now the standard replica technique is applied to perform the average of the logarithm in Eq. (3.37) via $\ln Z_N = \lim_{n\to 0} (Z_N^n - 1)/n$. In so doing we introduce hatted vectors $\hat{x} := (x^1, x^2, \ldots, x^n)$ for n-times replicated variables. Then specifying $A_{i,i'} := -(\hat{x}_i \cdot \hat{x}_{i'})/2$ in the characteristic function (3.33), we obtain for the disorder average

$$\begin{aligned} \langle [Z_N(\Omega)]^n \rangle &= \int_{\mathbb{R}^{Nn}} \left(\prod_{i=1}^{N} \frac{d\hat{x}_i}{(2\pi)^{n/2}} \right) \exp\left(-\frac{\Omega}{2} \sum_{i=1}^{N} \hat{x}_i^2 \right. \\ &\quad \left. + \frac{c}{N} \sum_{i,i'=1}^{N} e^{-(\hat{x}_i - \hat{x}_{i'})^2} - cN \right). \end{aligned} \tag{3.38}$$

Next we introduce a delta-correlated Gaussian random field $\psi: \mathbb{R}^n \to \mathbb{R}$, with zero mean, which serves to decouple the double sum over exponentials in the exponent of Eq. (3.38). This leads to the functional-integral representation

$$\langle [Z_N(\Omega)]^n \rangle = \int \mathcal{D}\psi \exp[-NF(\Omega, n, \psi)], \tag{3.39}$$

where

$$\begin{aligned} F(\Omega, n, \psi) &:= c + \frac{1}{2} \int_{\mathbb{R}^n} d\hat{x} [\psi(\hat{x})]^2 - \ln\left\{ \int_{\mathbb{R}^n} \frac{d\hat{x}}{(2\pi)^{n/2}} e^{-\Omega \hat{x}^2/2} \right. \\ &\quad \left. \times \exp\left[\sqrt{2c} \left(\frac{2}{\pi} \right)^{n/4} \int_{\mathbb{R}^n} d\hat{y}\, \psi(\hat{y}) e^{-(\hat{y}-\hat{x})^2} \right] \right\}. \end{aligned} \tag{3.40}$$

The saddle-point method is now applied to evaluate Eq. (3.39) in the limit $N \to \infty$, yielding $\langle [Z_N(\Omega)]^n \rangle \overset{N\to\infty}{\sim} \exp[-NF(\Omega, n, \tilde{\psi})]$, where $\tilde{\psi}$ is the unique solution of the saddle-point equation

$$\frac{\delta}{\delta\psi}F(\Omega,n,\psi)\big|_{\psi=\tilde{\psi}}=0. \tag{3.41}$$

Note that existence and uniqueness of $\tilde{\psi}$ are guaranteed, since for crosslink concentrations $0<c<\frac{1}{2}$ it is straightforward to prove that $F(\Omega,n,\psi)$ is strictly convex in the argument ψ. For the following it will be more advantageous to work with the Gaussian transform

$$\phi(\hat{x}):=\sqrt{2c}\left(\frac{2}{\pi}\right)^{n/4}\int_{\mathbb{R}^n}d\hat{y}\;\tilde{\psi}(\hat{y})e^{-(\hat{y}-\hat{x})^2} \tag{3.42}$$

of the solution $\tilde{\psi}$, in terms of which the saddle-point equation (3.41) is written as

$$\phi(\hat{x})=2c\,\frac{\int_{\mathbb{R}^n}d\hat{y}\;e^{-\Omega\hat{y}^2/2+\phi(\hat{y})}e^{-(\hat{x}-\hat{y})^2/2}}{\int_{\mathbb{R}^n}d\hat{y}\;e^{-\Omega\hat{y}^2/2+\phi(\hat{y})}}, \tag{3.43}$$

and the resolvent [Eq. (3.37)] reads

$$G(\Omega)=\lim_{n\to 0}\;\frac{1}{2n}\,\frac{\int_{\mathbb{R}^n}d\hat{y}\hat{y}^2e^{-\Omega\hat{y}^2/2+\phi(\hat{y})}}{\int_{\mathbb{R}^n}d\hat{y}\;e^{-\Omega\hat{y}^2/2+\phi(\hat{y})}}. \tag{3.44}$$

Note that Eq. (3.43) implies the normalization condition

$$\int_{\mathbb{R}^n}d\hat{x}\;\phi(\hat{x})=2c(2\pi)^{n/2}. \tag{3.45}$$

In order to compute the viscosity (3.35), Eqs. (3.43) and (3.44) have to be solved for small Ω after a continuation to $n=0$. We restrict ourselves to solutions ϕ of Eq. (3.43), which preserve rotational invariance in replica space and make the replica-symmetric ansatz

$$\phi(\hat{x})=\varphi_n^{\Omega}(\sqrt{\Omega}|\hat{x}|). \tag{3.46}$$

For later purposes the dependence on parameters has been made explicit. Introducing n-dimensional spherical coordinates, Eq. (3.44) transforms into

$$G(\Omega)=\lim_{n\to 0}\;\frac{1}{2n\Omega}\,\frac{\int_0^\infty d\rho\;\rho^{n+1}e^{-\rho^2/2+\varphi_n^{\Omega}(\rho)}}{\int_0^\infty d\rho\;\rho^{n-1}e^{-\rho^2/2+\varphi_n^{\Omega}(\rho)}}. \tag{3.47}$$

To proceed with Eq. (3.43), we employ an integral representation of the exponential of the n-dimensional Laplacian. More precisely, for any rotationally invariant function $f(|\hat{y}|)$ the identity

$$\int_{\mathbb{R}^n}\frac{d\hat{y}}{(2\pi\Omega)^{n/2}}\exp\left\{-\frac{1}{2\Omega}(\hat{x}-\hat{y})^2\right\}f(|\hat{y}|)$$
$$=\exp\left\{\frac{\Omega}{2}\left(\frac{d^2}{d\rho^2}+\frac{n-1}{\rho}\,\frac{d}{d\rho}\right)\right\}f(\rho)\Big|_{\rho=|\hat{x}|} \tag{3.48}$$

is valid for all $n\in\mathbb{N}$, and its application to Eq. (3.43) yields

$$\varphi_n^{\Omega}(\rho)=c(2\pi\Omega)^{n/2}\times\frac{\exp\left\{\frac{\Omega}{2}\left(\frac{d^2}{d\rho^2}+\frac{n-1}{\rho}\,\frac{d}{d\rho}\right)\right\}e^{-\rho^2/2+\varphi_n^{\Omega}(\rho)}}{s_n\int_0^\infty d\,\eta\;\eta^{n-1}e^{-\eta^2/2+\varphi_n^{\Omega}(\eta)}}. \tag{3.49}$$

Here $s_n:=n\pi^{n/2}/\Gamma(n/2+1)$ denotes the surface of the unit sphere in $\mathbb{R}^n$. The normalization (3.45) translates to

$$s_n\int_0^\infty d\rho\rho^{n-1}\varphi_n^{\Omega}(\rho)=2c(2\pi\Omega)^{n/2}. \tag{3.50}$$

Observing that $\lim_{n\to 0}[n\int_0^\infty d\rho\rho^{n-1}f(\rho)]=f(0)$ is valid for any sufficiently quickly decaying function f, we obtain from Eqs. (3.49) and (3.47)

$$\varphi_0^{\Omega}(\rho)=2ce^{-2c}\exp\left\{\frac{\Omega}{2}\left(\frac{d^2}{d\rho^2}-\frac{1}{\rho}\,\frac{d}{d\rho}\right)\right\}e^{-\rho^2/2+\varphi_0^{\Omega}(\rho)} \tag{3.51}$$

and

$$G(\Omega)=\frac{1}{2\Omega}e^{-2c}\int_0^\infty d\rho\;\rho e^{-\rho^2/2+\varphi_0^{\Omega}(\rho)}, \tag{3.52}$$

respectively. Here we made use of

$$\varphi_0^{\Omega}(0)=2c, \tag{3.53}$$

which is obtained from Eq. (3.50). The remaining task is to compute $\varphi_0^{\Omega}(\rho)$ up to first order in Ω, which, in turn, determines the $\mathcal{O}(1)$ contribution of $G(\Omega)$.

To this end we make the expansion

$$\varphi_0^{\Omega}(\rho)=\varphi_0^0(\rho)+g(\rho)\Omega+\mathcal{O}(\Omega^2), \tag{3.54}$$

insert it into Eq. (3.51), and equate the zeroth- and first-order terms

$$\varphi_0^0(\rho)=-W(-2ce^{-2c-\rho^2/2}), \tag{3.55}$$

$$g(\rho)=\{2[1-\varphi_0^0(\rho)]\}^{-1}\left(\frac{d^2}{d\rho^2}-\frac{1}{\rho}\,\frac{d}{d\rho}\right)\varphi_0^0(\rho). \tag{3.56}$$

Here W denotes the principal branch of the Lambert W-function [34], which is defined as the real solution of the transcendental equation

$$W(x)\exp[W(x)]=x,\quad x>-1/e. \tag{3.57}$$

Moreover, from inserting Eq. (3.54) into Eq. (3.52), we obtain the desired expansion

$$G(\Omega)=\frac{1}{4c}\int_0^\infty d\rho\;\rho\varphi_0^0(\rho)[\Omega^{-1}+g(\rho)]+\mathcal{O}(\Omega). \tag{3.58}$$

In order to calculate the integrals in Eq. (3.58), we employ the relation

$$\frac{d\varphi_0^0(\rho)}{d\rho} = -\frac{\rho\varphi_0^0(\rho)}{1-\varphi_0^0(\rho)}, \tag{3.59}$$

which follows from Eqs. (3.55) and (3.57). It helps to rewrite both the first term

$$\rho\varphi_0^0(\rho) = \frac{d}{d\rho}\left[\varphi_0^0(\rho)\left(\frac{1}{2}\varphi_0^0(\rho)-1\right)\right] \tag{3.60}$$

and, in combination with Eq. (3.56), the second term

$$\rho\varphi_0^0(\rho)g(\rho) = -\frac{1}{2}\frac{d}{d\rho}\left[\frac{1}{2}\left(\frac{d}{d\rho}\varphi_0^0(\rho)\right)^2 - \ln[1-\varphi_0^0(\rho)] - \varphi_0^0(\rho)\right] \tag{3.61}$$

of the integrand in Eq. (3.58). In addition, observing the normalization (3.53) and $(d\varphi_0^0/d\rho)(0)=0$, which also follows from Eq. (3.59), the evaluation of the integral in Eq. (3.58) leads to

$$G(\Omega) = \frac{1-c}{2\Omega} - \frac{1}{8c}[\ln(1-2c)+2c] + \mathcal{O}(\Omega). \tag{3.62}$$

Hence, the singular contributions for $\Omega\to 0$ cancel in Eq. (3.35), and we end up with the expression

$$\lim_{N\to\infty}\langle\eta\rangle = \frac{\zeta a^2}{8cd}\left[\ln\left(\frac{1}{1-2c}\right)-2c\right] \tag{3.63}$$

for the averaged viscosity, which coincides with the exact result (3.26) derived in Sec. III C.

We conclude that the replica trick and the assumption of replica symmetry provide an exact method to perform the disorder average in the random matrix ensemble (3.33) below the critical concentration. This was demonstrated for the viscosity, but we conjecture that it holds more generally, e.g. for the density of states.

IV. INTERMEDIATE INCOHERENT SCATTERING FUNCTION

Dynamic density fluctuations in polymer melts are encoded in the intermediate incoherent scattering function (2.11). The leading long-time behavior of its average $\langle S_t(q)\rangle$ over all crosslink realizations was computed in Ref. [8] for the ensemble (3.19) of uncorrelated crosslinks, for which $c_{\rm crit}=\frac{1}{2}$. Among others things, it was found that (1) the incoherent scattering function decays for all crosslink concentrations $0<c<c_{\rm crit}$ like a stretched exponential

$$\langle S_t(q)\rangle \overset{t\to\infty}{\sim} t^{-1/2}\exp\{-(t/t_q)^\alpha\} \quad \text{with} \quad \alpha=\frac{1}{2}, \tag{4.1}$$

where $t_q\sim q^{-2}$ is a diffusive time scale; (2) as the gelation transition is approached the diffusive time scale diverges,

$$q^2 t_q \overset{c\uparrow c_{\rm crit}}{\sim} (c_{\rm crit}-c)^{-\mu} \quad \text{with} \quad \mu=2, \tag{4.2}$$

and the effective diffusion constant vanishes linearly,

$$D_{\rm eff}^{-1} := \lim_{q\to 0} q^2\int_0^\infty dt\langle S_t(q)\rangle = D_0^{-1}\sum_{n=0}^\infty n^2\tau_n \overset{c\uparrow c_{\rm crit}}{\sim} (c_{\rm crit}-c)^{-y}, \tag{4.3}$$

where $y=1$ and $D_0:=(\zeta L)^{-1}$ is the bare diffusion constant; and (3) the incoherent scattering function decays algebraically at the critical point

$$\langle S_t(q)\rangle \overset{t\to\infty}{\sim} t^{-x} \quad \text{with} \quad x=\tfrac{1}{2}. \tag{4.4}$$

The analysis in Ref. [8] relies on the cluster decomposition (2.27) for $S_t(q)$ in the form of Eq. (2.31):

$$\langle S_t(q)\rangle = \sum_{n=0}^\infty n\tau_n\langle S_t(q)\rangle_n. \tag{4.5}$$

In addition, the plausible assumption has been used that the long-time asymptotics of $\langle S_t(q)\rangle$ is obtained by inserting the long-time asymptotics of $\langle S_t(q)\rangle_n$ into the right-hand side of Eq. (4.5).

The purpose of this section is twofold. First, for the case of uncorrelated crosslinks as in Ref. [8], we check whether the corrections to the leading long-time behavior of $\langle S_t(q)\rangle_n$ do not influence the leading long-time behavior of $\langle S_t(q)\rangle$, as assumed in Ref. [8]. This is done in Sec. IV B by asymptotic evaluations of an upper and a lower bound on $\langle S_t(q)\rangle$, which are constructed in Sec. IV A. Second, in Sec. IV C we determine the exponents α, μ, y, and x from the known critical exponents of random bond percolation by scaling relations. This generalizes the results in Ref. [8] to a non-mean-field distribution of crosslinks.

A. Upper and lower bound on $\langle S_t(q)\rangle$

Since the connectivity matrix Γ is positive semidefinite, the second exponential in Eq. (2.29) is bounded above by 1; hence

$$S_t(q) \leqslant \sum_{k=1}^K \frac{N_k}{N}\exp\left\{-\frac{q^2 t}{\zeta N_k L}\right\}. \tag{4.6}$$

For the computation of the crosslink average it is advantageous to reorder the sum according to Eq. (2.31):

$$\langle S_t(q)\rangle \leqslant \mathcal{U}_t(q) := \sum_{n=1}^\infty n\tau_n\exp\left\{-\frac{D_0 q^2 t}{n}\right\}. \tag{4.7}$$

A lower bound on $S_t(q)$ is obtained by neglecting the double-exponential contribution in Eq. (2.29):

$$S_t(q) \geqslant \sum_{k=1}^{K} \frac{N_k}{N} \exp\left\{ -\frac{q^2 t}{\zeta N_k L} \right\} \sum_{i \in \mathcal{N}_k} \sum_{s=1}^{L} \frac{1}{N_k L} \times \exp\left\{ -\frac{q^2 a^2}{d} \frac{1 - E_0(\mathcal{N}_k)}{\Gamma(\mathcal{N}_k)} (i,s;i,s) \right\}. \quad (4.8)$$

Next we apply the Jensen inequality to the right-hand side of Eq. (4.8) by replacing the normalized i and s sums over the exponentials by the exponential of the normalized sums. Together with Eq. (2.31), this yields

$$\langle S_t(q) \rangle \geqslant \sum_{n=1}^{\infty} n \tau_n \exp\left\{ -\frac{D_0 q^2 t}{n} \right\} \times \left\langle \exp\left\{ -\frac{q^2 a^2}{dnL} \mathrm{Tr}\left(\frac{1 - E_0}{\Gamma} \right) \right\} \right\rangle_n . \quad (4.9)$$

The lower bound is completed by yet another application of the Jensen inequality $\langle \exp(\bullet) \rangle_n \geqslant \exp(\langle \bullet \rangle_n)$, and the identification (2.26) of the resulting exponent with the viscosity

$$\langle S_t(q) \rangle \geqslant \mathcal{L}_t(q) := \sum_{n=1}^{\infty} n \tau_n \exp\left\{ -D_0 q^2 \left(\frac{t}{n} + 2 \langle \eta \rangle_n \right) \right\}. \quad (4.10)$$

In summary, we have found the chain of inequalities

$$\mathcal{L}_t(q) \leqslant \langle S_t(q) \rangle \leqslant \mathcal{U}_t(q). \quad (4.11)$$

B. Uncorrelated crosslinks

It was argued in Ref. [8] that $\langle S_t(q) \rangle_n \overset{t \to \infty}{\sim} \exp\{-D_0 q^2 t/n\}$. This relation follows from Eq. (2.29). Assuming that the corrections to this leading behavior do not play a rôle in the cluster decomposition (4.5), the Kohlrausch law

$$\langle S_t(q) \rangle \overset{t \to \infty}{\sim} \sum_{n=0}^{\infty} n \tau_n \exp\{-D_0 q^2 t/n\} \overset{t \to \infty}{\sim} \frac{1}{(8c^2 D_0 q^2 t)^{1/2}} \exp\{-2[h(c) D_0 q^2 t]^{1/2}\}, \quad (4.12)$$

$0 < c \leqslant 1/2$, was found [8] which yields the critical exponents in Eqs. (4.1)–(4.4). Here we introduced the function $h(c) := 2c - 1 - \ln(2c)$, and observed $h(c) \sim (c_{\mathrm{crit}} - c)^2$ for $c \uparrow_{\mathrm{crit}}$. In order to derive the second line in Eq. (4.12), the explicit form (3.20) of τ_n in the case of uncorrelated crosslinks was used, $n!$ was replaced by its Stirling asymptotics, and the sum over n by an integral, whose evaluation yielded the result.

In this subsection we want to confirm that the corrections to the asymptotic behavior of $\langle S_t(q) \rangle_n$ do not influence the Kohlrausch law (4.12). To do so we employ bounds (4.11). We also perform a more careful evaluation of the sums over the cluster sizes n, than the one which was used in Ref. [8] to derive the second line in Eq. (4.12). Details of this calculation are deferred to the Appendix.

We start with the upper bound (4.7), which in the notation (A1) of the Appendix reads $\mathcal{U}_t(q) = F(0, D_0 q^2 t)$. Therefore we conclude from Eq. (A19) that

$$\lim_{q^2 t \to \infty} \frac{\mathcal{U}_t(q)}{(8c^2 D_0 q^2 t)^{-1/2} \exp\{-2[h(c) D_0 q^2 t]^{1/2}\}} = 1. \quad (4.13)$$

This result also confirms the previously obtained asymptotic equality in the second line of Eq. (4.12).

As to the lower bound (4.10), we first recall the expression (3.31) for $\langle \eta \rangle_n$ and the inequality $\langle \eta \rangle_n |_{L=1} \leqslant b \sqrt{n}$, which follows from Eqs. (3.23) and (3.22), with $b > 0$ being a finite constant. Again in the notation (A1) of the Appendix, this yields

$$\mathcal{L}_t(q) \geqslant e^{-B_1 q^2} F(q^2 B_2, D_0 q^2 t), \quad (4.14)$$

where $B_1 := D_0 \zeta l^2 L \mathcal{Q}_L / (2d)$ and $B_2 := D_0 b \zeta a^2 L (1 + \mathcal{Q}_L l^2 / a^2)/(2d)$. Consequently, Eq. (A20) implies

$$\lim_{\substack{q^2 t \to \infty \\ q^6 t \to 0}} \frac{\mathcal{L}^t(q)}{(8c^2 D_0 q^2 t)^{-1/2} \exp\{-2[h(c) D_0 q^2 t]^{1/2}\}} \geqslant 1. \quad (4.15)$$

Taken together, Eqs. (4.13) and (4.15) provide us with the equality

$$\lim_{\substack{q^2 t \to \infty \\ q^6 t \to 0}} \frac{\langle S_t(q) \rangle}{(8c^2 D_0 q^2 t)^{-1/2} \exp\{-2[h(c) D_0 q^2 t]^{1/2}\}} = 1. \quad (4.16)$$

In other words, the bounds (4.11) only confirm the previously obtained Kohlrausch law (4.12), if one also considers the limit of small momentum transfer—as may be a reasonable approximation for an experimental low-angle-scattering situation. Nevertheless, we believe that the stretched exponential (4.12) reflects the true long-time asymptotics of $\langle S_t(q) \rangle$ for finite q, as well, and that the lower bound (4.10) is not sharp enough to reproduce this.

On the other hand the bounds (4.11) are sharp enough to establish the expression

$$D_{\mathrm{eff}}^{-1} = D_0^{-1} \sum_{n=0}^{\infty} n^2 \tau_n = \frac{1}{D_0 (1 - 2c)} \quad (4.17)$$

for the effective diffusion constant D_{eff}. The first equality was already stated in Eq. (4.3). The second follows for $0 < c < 1/2$ by differentiating the relation $1 = \Sigma_{n=1}^{\infty} n \tau_n$ with respect to the crosslink concentration c. Obviously, the result is in accordance with $y = 1$ in Eq. (4.3). The linear dependence of D_{eff} on c is displayed in Fig. 1.

C. Scaling description

In this subsection we extend the results of Ref. [8] to the crosslink statistics generated by d-dimensional random bond percolation, whose basic properties were recalled in Sec. III B.

For the case of uncorrelated crosslinks, we saw in Ref. [8]—and confirmed in Sec. IV B by alternative methods—that the critical exponents (4.1)–(4.4) of the Kohlrausch law (4.12) do not depend on the number L of monomers per polymer. Therefore we restrict ourselves to the case $L=1$ of Brownian particles in the following. The results of the last subsection also motivate us to replace $\langle S_t(q)\rangle_n$ by its long-time asymptotics in Eq. (4.5), that is,

$$\langle S_t(q)\rangle \overset{t\to\infty}{\sim} \sum_{n=0}^{\infty} n\,\tau_n \exp\{-D_0 q^2 t/n\}. \tag{4.18}$$

For $t\to\infty$ this series is expected to be dominated by terms with large n. Therefore we insert the scaling law (3.6) for τ_n in Eq. (4.18), and use the fact that the associated scaling function f decays exponentially for large n. Up to a constant this yields

$$\langle S_t(q)\rangle \overset{t\to\infty}{\sim} \sum_{n=0}^{\infty} n^{1-\tau} \exp\{-(c_{\rm crit}-c)^{1/\sigma} n - D_0 q^2 t/n\}. \tag{4.19}$$

In order to proceed, we replace the sum over n in Eq. (4.19) by the integral

$$\int_0^{\infty} dn\, n^{1-\tau} \exp\{-(c_{\rm crit}-c)^{1/\sigma} n - D_0 q^2 t/n\}, \tag{4.20}$$

which should not affect the long-time asymptotics either. Using formula 3.471.9 in Ref. [29], we then express the integral in Eq. (4.20) in terms of a Bessel function. Its asymptotic expansion according to formula 8.451.6 in Ref. [29] finally gives, up to a constant,

$$\langle S_t(q)\rangle \overset{t\to\infty}{\sim} \frac{(c_{\rm crit}-c)^{(2\tau-5)/(4\sigma)}}{(D_0 q^2 t)^{(2\tau-3)/4}} \times \exp\{-2[D_0 q^2 (c_{\rm crit}-c)^{1/\sigma} t]^{1/2}\} \tag{4.21}$$

for $c<c_{\rm crit}$. For $c=c_{\rm crit}$ we conclude

$$\langle S_t(q)\rangle \overset{t\to\infty}{\sim} \frac{\text{const}}{(D_0 q^2 t)^{\tau-2}} \tag{4.22}$$

directly from Eq. (4.20). Hence we find $\alpha=\frac{1}{2}$ for the critical exponent (4.1), the same value as was found for uncorrelated crosslinks. In contrast, the exponents defined by relations (4.2)–(4.4) turn out to be different. More precisely, we obtain the scaling relations

$$\mu = 1/\sigma \approx 2.22, \tag{4.23}$$

$$y = (3-\tau)/\sigma \approx 1.82, \tag{4.24}$$

$$x = \tau - 2 \approx 0.18. \tag{4.25}$$

The approximate numerical values are those for random bond percolation in three dimensions [7]. A discussion of these results in comparison to the experimental data will be given in Sec. V.

V. CONCLUDING REMARKS

Starting from a Rouse model of a crosslinked polymer melt, we discuss the critical dynamics of the gelation transition with particular emphasis on the static shear viscosity and the long-time behavior of the incoherent scattering function. Our main result is an exact relation for the critical exponent of the viscosity,

$$k = \phi - \beta, \tag{5.1}$$

in terms of the crossover and thermal exponents of percolation theory. Two crosslink distributions have been analyzed in detail: one corresponding to a mean-field percolation model and one corresponding to finite-dimensional percolation. For the first distribution we were able to derive the exact expression (3.32) for the static shear viscosity. This result is valid for all crosslink concentrations $0<c<c_{\rm crit}=\frac{1}{2}$, and exhibits a logarithmic divergence at the critical crosslink concentration $c_{\rm crit}$, that is, $k=0$. The critical exponent $k=0$ also follows from the scaling relation (5.1) when inserting the mean-field values $\phi=1$, see e.g., Ref. [27], and $\beta=1$. For the second crosslink distribution the scaling relation (5.1) can either be evaluated in terms of the $\epsilon=6-d$ expansion [27] for ϕ and β, yielding $k=\epsilon/6+11\epsilon^2/1764+\mathcal{O}(\epsilon^3)$. Alternatively, one may insert the numerical value of ϕ known from high-precision simulations of random resistor networks in $d=3$ dimensions [35], which, together with the corresponding value for β gives $k|_{d=3}\approx 0.71$.

The experimental values for k are systematically larger. Early experiments by Adam *et al.* [3] were performed near the gelation threshold of polycondensation reactions. For the samples with low molecular weight, data for the viscosity were fitted to a power-law divergence with exponent $k=0.8\pm0.1$. On the other hand, the viscosity data of samples with high molecular weight could not be fitted to a power-law divergence. Considerably larger exponent values were observed in more recent experiments on silica gels and epoxy raisins. Colby *et al.* [36] reported values $1.4\leqslant k\leqslant 1.7$, and Martin *et al.* obtained $k=1.4\pm0.2$ from viscoelastic measurements [37] and $k=1.5\pm0.2$ rather indirectly from measurements of the incoherent scattering function [2]. The origin of the scatter of the experimental data is not clear. A splitting of the static universality class into different dynamic ones has been suggested [3]. Another possible explanation is the size of the critical region, which is expected to depend on chain length [38]. The observed range of exponent values could then be interpreted as a crossover from mean-field to critical behavior.

What are the shortcomings of our theory? We have written the average macroscopic viscosity as a weighted sum of

contributions from individual clusters. Such a decomposition holds exactly within the Rouse model of a crosslinked melt, but is expected to be valid more generally—as long as there are no interactions between different clusters. Retaining the cluster decomposition, the only unknown is the contribution of an individual cluster, because the distribution of clusters should indeed be given by percolation theory, and hence is known to high precision. As far as single clusters are concerned, we expect that relaxation times are longest for Rouse dynamics. If, for example, we were to use Zimm dynamics together with a preaveraging approximation, we would find shorter relaxation times as compared to the Rouse model, and hence even smaller values of k. This suggests that the discrepancy between theory and experiment cannot be cured, if we retain the cluster decomposition. Hydrodynamic interactions, excluded-volume interactions, and entanglement effects all invalidate the cluster decomposition. One expects entanglement effects to play a vital role in stress relaxation [15]. However, the static viscosity measures stress relaxation only on the longest time scales in the sol phase. It was argued [36,39] that in the regime close to the transition, entanglement effects are less important for two reasons: first, there are almost no permanent entanglements in the sense of interlocking loops; second, the time scale of a temporary entanglement of two clusters is determined by the smaller cluster, whereas the dynamics on the longest time scales is determined by the larger cluster. From calculations of static quantities we know that the excluded-volume interaction is essential for the stability of the network in the gel phase [40]. In the sol phase, on the other hand, the role of the excluded-volume interaction is less transparent. On one hand, the $\epsilon = 6-d$ expansion for a gelation model with excluded-volume interactions [41] yields the same critical exponents as obtained from the ϵ expansion of percolation theory [7]. On the other hand, the excluded-volume interaction is known to be relevant [42] for static and dynamic properties of polymer melts and solutions below $d=4$.

The decay of density fluctuations in silica gels has been investigated by quasi elastic light scattering [2]. In the sol phase, a stretched exponential of the autocorrelation was observed, $S_t(q) \sim \exp\{-(t/t_q)^{\alpha}\}$ with $\alpha = 0.65 \pm 0.05$. The experimentally determined time scale t_q is diffusive and diverges as the gelation transition is approached $t_q \sim (c_{\mathrm{crit}} - c)^{-2.2}$. The critical behavior of the diffusion constant was determined as well and in particular the exponent value $y = 1.9 \pm 0.1$ was found. At the critical point, the scattering experiments reveal an algebraic decay in time of $S_t(q)$ with an exponent $x = 0.135 \pm 0.015$. All these findings are in qualitative agreement with our theory. In fact our expression (2.29) for $S_t(q)$ has been suggested on phenomenological grounds as a starting point for the discussion of the critical dynamics at the sol-gel transition [10]. The exponent values of mean-field theory, see Eqs. (4.1)–(4.4), deviate from the experimental ones, as one would expect. If we use the scaling description of finite-dimensional percolation, then the exponent α of the stretched exponential is unchanged. Its value, $\alpha = \frac{1}{2}$, is characteristic of Rouse dynamics and independent of cluster statistics. The corrections to the other exponents go in the right direction; see Eqs. (4.23)–(4.25). However, discrepancies beyond the experimental error bars remain and are probably due to our neglect of excluded-volume and hydrodynamic interactions.

Our approach can be extended to study stress relaxation at finite frequencies. Within the Rouse model, the dynamics is completely determined by the eigenvalue spectrum of the random connectivity matrix Γ. For the mean-field distribution of crosslinks its eigenvalue spectrum can be computed with the replica trick [31], so that stress relaxation at finite frequencies becomes accessible to analytical theory. Work along these lines is in progress.

ACKNOWLEDGMENTS

This work was supported by the DFG through SFB 345. K.B. acknowledges financial support by the DFG under Grant No. Br 1894/1-1.

APPENDIX: EVALUATION OF THE BOUNDS (4.11)

Here we present some technical details which are needed in the asymptotic evaluation for $t \to \infty$ of the bounds (4.11) on the averaged intermediate incoherent scattering function $S_t(q)$. The quantity of interest is the series

$$F(B,T) := \sum_{n=1}^{\infty} n \tau_n e^{-T/n} e^{-B\sqrt{n}}, \tag{A1}$$

where $B \geqslant 0$, $T > 0$ and $\tau_n = n^{n-2} e^{-nh(c)}/(2cn!e^n)$ follows from Eq. (3.20) with $h(c) := 2c - 1 - \ln(2c)$. Now pick a natural number P, split the series in two parts given by the first $P-1$ terms and the terms with $n \geqslant P$, respectively, and apply the Stirling approximation, Eq. (6.1.58) in Ref. [43],

$$n! = (2\pi)^{1/2} n^{n+1/2} \exp\{-n + \theta(n)/(12n)\}, \tag{A2}$$

$0 < \theta(n) < 1$, to the terms with $n \geqslant P$. Thus we infer the existence of a constant

$$e^{-1/(12P)} \leqslant u_p \leqslant 1, \tag{A3}$$

such that

$$F(B,T) = R_P(B,T) + \frac{u_P}{2c(2\pi)^{1/2}} \tilde{F}(B,T), \tag{A4}$$

where

$$R_P(B,T) := \sum_{n=1}^{P-1} \left(n\tau_n - \frac{u_P}{2c(2\pi)^{1/2} n^{3/2}} e^{-nh(c)} \right) e^{-T/n} e^{-B\sqrt{n}} \tag{A5}$$

and

$$\tilde{F}(B,T) := \sum_{n=1}^{\infty} n^{-3/2} \exp\{-nh(c) - T/n - B\sqrt{n}\}. \tag{A6}$$

Note that

$$|R_P(B,T)| \leqslant e^{-T/(P-1)} \sum_{n=1}^{P-1} \left| n\tau_n - \frac{u_P e^{-nh(c)}}{2c(2\pi)^{1/2} n^{3/2}} \right| \tag{A7}$$

decays exponentially for $T \to \infty$, uniformly in $B \geqslant 0$.

In order to proceed with $\tilde{F}(B,T)$ we use the Fourier representation

$$e^{-\alpha/2} = \int_{\mathbb{R}} dx e^{ix} \frac{e^{-x^2/(2\alpha)}}{(2\pi\alpha)^{1/2}}, \quad \alpha > 0, \tag{A8}$$

and arrive at

$$\tilde{F}(B,T) = \int_{\mathbb{R}} \frac{dx}{(4\pi D_0 t)^{1/2}} e^{ix} \int_{A(x)}^{\infty} d\lambda \sum_{n=1}^{\infty} e^{-\lambda n} e^{-B\sqrt{n}}, \tag{A9}$$

where $A(x) := h(c) + x^2/(4T)$. According to Eq. (11.1.1) in Ref. [44] the series in Eq. (A9) admits an integral representation such that

$$\tilde{F}(B,T) = \frac{B}{4\pi T^{1/2}} \int_{\mathbb{R}} dx e^{ix} \int_{A(x)}^{\infty} d\lambda \int_0^{\infty} d\xi \frac{e^{-B^2/(4\xi)}}{\xi^{3/2}(e^{\xi+\lambda}-1)}. \tag{A10}$$

After a partial integration with respect to x and the subsequent changes-of-variables $z := x(4T)^{-1/2}$ and $\zeta := (2\xi)^{-1/2}$, Eq. (A10) reads

$$\tilde{F}(B,T) = \frac{-i}{(\pi T)^{1/2}} \int_{\mathbb{R}} d\zeta \frac{e^{-\zeta^2/2}}{(2\pi)^{1/2}} \int_{\mathbb{R}} dz \frac{z e^{2iz\sqrt{T}}}{e^{z^2 + h(c,B/\zeta)} - 1}, \tag{A11}$$

with $h(c,r) := h(c) + r^2/2$. The z-integration can be done with the help of the residue theorem. To this end we close the integration contour with a semicircle in the complex upper half-plane and remark that the integrand has simple poles $z_n(B/\zeta) := z_n'(B/\zeta) + iz_n''(B/\zeta)$, $n \in \mathbb{Z}$, in this half-plane, whose real and imaginary parts are given by

$$z_n'(r) := \frac{\mathrm{sgn}(n)}{\sqrt{2}} \{ \sqrt{[h(c,r)]^2 + (2\pi n)^2} - h(c,r) \}^{1/2}, \tag{A12}$$

$$z_n'' := \frac{1}{\sqrt{2}} \{ \sqrt{[h(c,r)]^2 + (2\pi n)^2} + h(c,r) \}^{1/2}.$$

Hence we find

$$\tilde{F}(B,T) = \left(\frac{\pi}{T} \right)^{1/2} \int_{\mathbb{R}} d\zeta \frac{e^{-\zeta^2/2}}{(2\pi)^{1/2}} \times [e^{-2[Th(c,B/\zeta)]^{1/2}} + 2\tilde{F}_1(B/\zeta, T)], \tag{A13}$$

where

$$\tilde{F}_1(r,T) := \sum_{n=1}^{\infty} e^{-2z_n''(r)\sqrt{T}} \cos[2z_n'(r)\sqrt{T}]. \tag{A14}$$

Using $z_n''(r) \geqslant z_n''(0)$, we obtain the r-independent upper bound

$$|\tilde{F}_1(r,T)| \leqslant e^{-2z_1''(0)\sqrt{T}} \sum_{n=1}^{\infty} e^{-2[z_n''(0) - z_1''(0)]\sqrt{T}}$$

$$\leqslant f e^{-2z_1''(0)\sqrt{T}}. \tag{A15}$$

Here f is a uniform constant for all $T \geqslant T_0 > 0$, because $z_n''(0) > z_1''(0)$ for $n > 1$ and $z_n''(0) \sim n^{1/2}$ for $n \to \infty$. Thus we conclude from Eqs. (A4), (A7), (A13), and (A15) that

$$\lim_{T\to\infty} \frac{F(0,T)}{(8c^2T)^{-1/2} \exp\{-2[h(c)T]^{1/2}\}} = u_P \tag{A16}$$

holds for all $P \in \mathbb{N}$.

For $B > 0$ the inequality $\sqrt{h(c,r)} \leqslant \sqrt{h(c)} + 2^{-1/2}|r|$ leads to the lower bound

$$\int_{\mathbb{R}} d\zeta \frac{e^{-\zeta^2/2}}{(2\pi)^{1/2}} e^{-2[Th(c,B/\zeta)]^{1/2}} \geqslant e^{-2[Th(c)]^{1/2}} \int_{\mathbb{R}} d\zeta \frac{e^{-\zeta^2/2}}{(2\pi)^{1/2}} e^{-(2B^2T)^{1/2}/|\zeta|}. \tag{A17}$$

This bound, together with the same arguments which led to Eq. (A16), now yield

$$\lim_{\substack{T\to\infty \\ B^2T\to 0}} \frac{F(B,T)}{(8c^2T)^{-1/2} \exp\{-2[h(c)T]^{1/2}\}} \geqslant u_P \tag{A18}$$

for all $P \in \mathbb{N}$. Letting $P \to \infty$, and observing Eqs. (A3), (A16), and (A18), respectively, implies

$$\lim_{T\to\infty} \frac{F(0,T)}{(8c^2T)^{-1/2} \exp\{-2[h(c)T]^{1/2}\}} = 1 \tag{A19}$$

and

$$\lim_{\substack{T\to\infty \\ B^2T\to 0}} \frac{F(B,T)}{(8c^2T)^{-1/2} \exp\{-2[h(c)T]^{1/2}\}} \geqslant 1. \tag{A20}$$

[1] J. E. Martin and D. Adolf, Annu. Rev. Phys. Chem. **42**, 311 (1991).
[2] J. E. Martin and J. Wilcoxon, Phys. Rev. Lett. **61**, 373 (1988); D. Adolf and J. E. Martin, Macromolecules **23**, 3700 (1990); J. E. Martin, J. Wilcoxon, and J. Odinek, Phys. Rev. A **43**, 858 (1991).
[3] M. Adam, M. Delsanti, D. Durand, G. Hild, and J. P. Munch, Pure Appl. Chem. **53**, 1489 (1981); M. Adam, M. Delsanti, and D. Durand, Macromolecules **18**, 2285 (1985).
[4] K. Vollmayr, W. Kob, and K. Binder, J. Chem. Phys. **105**, 4714 (1996).
[5] D. Stauffer, A. Coniglio, and M. Adam, Adv. Polym. Sci. **44**, 103 (1982).
[6] P.-G. de Gennes, C. R. Acad. Sci. (Paris) **286B**, 131 (1978).
[7] D. Stauffer and A. Aharony, *Introduction to Percolation Theory*, revised 2nd ed. (Taylor and Francis, London, 1994); A. Bunde and S. Havlin, in *Fractals and Disordered Systems*, edited by A. Bunde and S. Havlin (Springer, Berlin, 1996), pp. 59 and 115.
[8] K. Broderix, P. M. Goldbart, and A. Zippelius, Phys. Rev. Lett. **79**, 3688 (1997).
[9] M. E. Cates, J. Phys. (Paris) **46**, 1059 (1985).
[10] P.-G. de Gennes, J. Phys. (Paris) Lett. **40**, L-197 (1979).
[11] J. P. Straley, Phys. Rev. B **15**, 5733 (1977).
[12] A. B. Harris and T. C. Lubensky, Phys. Rev. B **35**, 6964 (1987).
[13] M. P. Solf and T. A. Vilgis, J. Phys. A **28**, 6655 (1995).
[14] K. Broderix, H. Löwe, P. Müller, and A. Zippelius, Europhys. Lett. **48**, 421 (1999).
[15] M. Doi and S. F. Edwards, *The Theory of Polymer Dynamics* (Clarendon Press, Oxford, 1985).
[16] R. B. Bird, C. F. Curtiss, R. C. Armstrong, and O. Hassager, *Dynamics of Polymeric Liquids*, 2nd ed. (Wiley, New York, 1987), Vol. 2.
[17] P. Erdős and A. Rényi, Magyar Tud. Akad. Mat. Kut. Int. Kőzl. **5**, 17 (1960); reprinted in *The Art of Counting*, edited by J. Spencer (MIT Press, Cambridge, MA, 1973).
[18] M. J. Stephen, Phys. Rev. B **15**, 5674 (1977).
[19] A. E. Albert, *Regression and the Moore-Penrose Pseudoinverse* (Academic, New York, 1972).
[20] B. Bollobás, *Modern Graph Theory* (Springer, New York, 1998).
[21] D. J. Klein and M. Randić, J. Math. Chem. **12**, 81 (1993).
[22] P. J. Flory, J. Am. Chem. Soc. **63**, 3083 (1941); **63**, 3091 (1941); **63**, 3096 (1941); J. Phys. Chem. **46**, 132 (1942).
[23] W. H. Stockmayer, J. Chem. Phys. **11**, 45 (1943); **12**, 125 (1944).
[24] P. J. Flory, *Principles of Polymer Chemistry*, 15th printing (Cornell University Press, Ithaca, NY, 1992).
[25] D. Stauffer, J. Chem. Soc. Faraday Trans. 2 **72**, 1354 (1976).
[26] T. C. Lubensky and J. Wang, Phys. Rev. B **33**, 4998 (1985).
[27] O. Stenull, H. K. Janssen, and K. Oerding, Phys. Rev. E **59**, 4919 (1999).
[28] A. Meir and J. W. Moon, J. Comb. Theory **8**, 99 (1970).
[29] I. S. Gradshteyn and I. M. Rhyzik, *Table of Integrals, Series, and Products* (Academic, New York, 1980).
[30] B. Bollobás, *Random Graphs* (Academic, London, 1985).
[31] G. J. Rodgers and A. J. Bray, Phys. Rev. B **37**, 3557 (1988); A. J. Bray and G. J. Rodgers, *ibid.* **38**, 11 461 (1988).
[32] G. Biroli and R. Monasson, J. Phys. A **32**, L255 (1999).
[33] A. Cavagna, I. Giardina, and G. Parisi, Phys. Rev. Lett. **83**, 108 (1999).
[34] R. M. Corless, G. H. Gonnet, D. E. G. Haare, D. J. Jeffrey, and D. E. Knuth, Adv. Comput. Math. **5**, 329 (1996).
[35] D. B. Gingold and D. J. Lobb, Phys. Rev. B **42**, 8220 (1990).
[36] R. H. Colby, J. R. Gillmor, and M. Rubinstein, Phys. Rev. E **48**, 3712 (1993).
[37] J. E. Martin, D. Adolf, and J. Wilcoxon, Phys. Rev. Lett. **61**, 2620 (1988).
[38] P.-G. de Gennes, J. Phys. (Paris) Lett. **38**, L-355 (1977).
[39] M. Rubinstein, S. Zurek, T. C. B. McLeish, and R. C. Ball, J. Phys. (Paris) **51**, 757 (1990); S. T. Milner, T. C. B. McLeish, R. N. Young, A. Hakiki, and J. M. Johnson, Macromolecules **31**, 9345 (1998).
[40] P. M. Goldbart, H. Castillo, and A. Zippelius, Adv. Phys. **45**, 393 (1996).
[41] W. Peng and P. M. Goldbart, Phys. Rev. E **61**, 3339 (2000).
[42] L. Schäfer, *Excluded Volume Effects in Polymer Solutions* (Springer, Berlin, 1999).
[43] M. Abramowitz and I. A. Stegun, *Handbook of Mathematical Functions with Formulas, Graphs and Mathematical Tables*, 9th printing (Dover, New York, 1972).
[44] E. R. Hansen, *A Table of Series and Products* (Prentice-Hall, Englewood Cliffs, NJ, 1975).